
Janus van der Waals equations for real molecules with two-sided phase transitions

Jihwan Kim¹, Do-Hyun Kim^{2,*}, and Jeong-Hyuck Park^{1,*}

¹*Department of Physics, Sogang University
35 Baekbeom-ro, Mapo-gu, Seoul 04107, Korea*

²*Institute for Whole Person Education, Sogang University
35 Baekbeom-ro, Mapo-gu, Seoul 04107, Korea*

*Co-correspondence: dohyunkim@sogang.ac.kr & park@sogang.ac.kr

ABSTRACT

We obtain families of generalised van der Waals equations characterised by an even number $n = 2, 4, 6$ and a continuous free parameter which is tunable for a critical compressibility factor. Each equation features two adjacent critical points which have a common critical temperature T_c and arbitrarily close two critical densities. The critical phase transitions are naturally two-sided: the critical exponents are $\alpha_P = \gamma_P = \frac{2}{3}$, $\beta_P = \delta^{-1} = \frac{1}{3}$ for $T > T_c$ and $\alpha_P = \gamma_P = \frac{n}{n+1}$, $\beta_P = \delta^{-1} = \frac{1}{n+1}$ for $T < T_c$. In contrast with the original van der Waals equation, our novel equations all reduce consistently to the classical ideal gas law in low density limit. We test our formulas against NIST data for eleven major molecules and show agreements better than the original van der Waals equation, not only near to the critical points but also in low density regions.

Keywords: Equations of State, van der Waals Equation, Critical Point, Two-sided Phase Transition, NIST Reference Data, Analyticity

1 INTRODUCTION

Two-sided phase transitions are rather out of the ordinary critical phenomena as their critical exponents take different values in the higher and the lower temperature phases. While the general renormalization group argument, *e.g.* [1], might appear to suppress such an unusual bilateral critical behaviour, they have been reported to occur in various systems, such as isotropic ferromagnet [2], XY-Heisenberg model [3], complex Sachdev-Ye-Kitaev models [4], and liquid-gas transitions of real molecules [5]. To explain the two-sided critical phase transitions, while respecting the analyticity of the canonical partition function of a finite system, it was hypothesized that there may exist not a single but double critical points which should be quite close to each other [5].

It is the dual-purpose of the present paper to modify the van der Waals equation toward the description of the two-sided phase transitions and to test our novel formulas against NIST Reference

Data (RRID:SCR_006452) [6], specifically for eleven real molecules. Our proposed equations of state, which we dub *Janus van der Waals equations*,¹ are characterised by extremely adjacent two critical points. The two critical points share strictly the same critical temperature, T_c , but, remarkably, the critical pressure, P_c , and the critical volume per particles, v_c , differ by arbitrarily small amounts, such that the distinct two critical points can appear practically indistinguishable.

The (original) van der Waals equation of state,

$$\left(P_r + \frac{3}{v_r^2}\right) \left(v_r - \frac{1}{3}\right) = \frac{8}{3}T_r, \quad (1)$$

was meant to be an improvement of the classical ideal gas law, *i.e.*

$$Pv = k_B T \quad \iff \quad P_r v_r = \chi T_r \quad : \quad \chi = \frac{k_B T_c}{P_c v_c}, \quad (2)$$

by attempting to take into account the finite volume of molecules and intermolecular attractions. In (1), (2), and henceforth, $P_r = P/P_c$, $T_r = T/T_c$, and $v_r = v/v_c$ are the reduced pressure, temperature, and volume per particle respectively, while $\chi = k_B T_c / (P_c v_c)$ denotes the inverse of the critical compressibility factor which is dimensionless. The critical point is given by $P_r = T_r = v_r = 1$, such that, the van der Waals equation (1) contains the critical point as $(1 + 3)(1 - \frac{1}{3}) = \frac{8}{3}$, and may describe the near critical behaviour. However, in a large volume or low density limit, Eq.(1) gives

$$Pv \simeq \left(\frac{8P_c v_c}{3T_c}\right) T \neq k_B T. \quad (3)$$

Thus, unless $\chi = \frac{8}{3}$ by chance, the van der Waals equation (1) cannot reduce to the classical ideal gas law (2) in the low density limit, and accordingly fails to describe real gases at low densities. In fact, experimental real values of χ are typically around 3.5 larger than $\frac{8}{3}$. In contrast, our proposed Janus van der Waals equations are going to be consistent with the classical ideal gas law (2) at low densities. They are not particularly motivated by the finite volume or intermolecular effects. Rather, we address directly the definition of the critical point in thermodynamics: for a given equation of state, a critical point can be identified as a stationary inflection point in the constant temperature line on a pressure *versus* volume diagram. Specifically for a certain natural number greater than or equal to two, $n_c \geq 2$, we have at the critical point,

$$\frac{\partial^k P(T_c, v_c)}{\partial v^k} = 0 \quad \text{for} \quad 1 \leq k \leq n_c, \quad (4)$$

while the next higher order derivative having $k = n_c + 1$ is nontrivial. In particular for the van der Waals equation (1), the number takes the minimal value $n_c = 2$ and its spinodal curve that is by definition the lowest order $k = 1$ in (4) is given by

$$T_r = 1 - \frac{(v_r - 1)^2(4v_r - 1)}{4v_r^3}. \quad (5)$$

This expression shows clearly that on the spinodal curve the temperature is locally maximal at the critical point. In general, the characteristic number n_c can differ from two and may be used to classify the critical

¹ 'Janus' is a Roman god who has two faces. Our nomenclature is inspired partially by [7].

points, being dubbed as ‘critical index’ [5]. Thoroughly from (4), both the critical isobar of $P_r \equiv 1$ and the spinodal curve satisfy simple power-law behaviors around the critical point,

$$T - T_c \propto (v - v_c)^{1+n_c} : \text{critical isobar}, \quad T - T_c \propto (v - v_c)^{n_c} : \text{spinodal curve}. \quad (6)$$

Combined with the analyticity of the underlying canonical partition function, this result fixes the (isobaric) critical exponents [8], $\alpha_P = \gamma_P = \frac{n_c}{1+n_c}$ and $\beta_P = \delta^{-1} = \frac{1}{1+n_c}$. These satisfy Rushbrooke and Widom scaling laws. Since $n_c \geq 2$, the two curves of (6) are actually tangent to each other at the critical point.

The main result of [5] was that the NIST Reference Data of twenty major molecules [6] are indeed consistent with the analytic prediction of the critical exponents, and moreover that the critical phase transitions are remarkably two-sided: for $T > T_c$ the critical index is 2 universally, yet for $T < T_c$ it varies as $n \equiv 2, 3, 4, 5, 6$ depending on each molecule, collectively denoted by a pair of critical indices, $n_c \Rightarrow (n_+, n_-) = (2, n)$. In this work, we present Janus van der Waals equations characterised by a pair of adjacent critical points with indices $(n_+, n_-) = (2, n)$ for $n = 2, 4, 6$ (even). With one continuous input parameter which will be chosen to match the critical compressibility, they are shown to describe remarkably well all the real molecules with even critical indices identified in [5]. They are cyclopentane (C_5H_{10}) for $n = 2$; nitrogen (N_2), argon (Ar), methane (CH_4), ethylene (C_2H_4), ethane (C_2H_6), propylene (C_3H_6), propane (C_3H_8), butane (C_4H_{10}), and isobutane (C_4H_{10}) for $n = 4$; and helium-4 (4He) for $n = 6$.

2 ANSATZ AND DERIVATION

Our Janus van der Waals equations assume an ansatz,

$$\left(P_r + \chi f_n(v_r) \right) (v_r - b) = \chi T_r, \quad (7)$$

where $f_n(v_r)$ is supposed to be a polynomial in v_r^{-1} and $\chi = \frac{k_B T_c}{P_c v_c}$ is the (experimentally determinable) genuine *free* parameter which will guarantee the consistency with the classical ideal gas law (2) in the large volume limit, hence resolving the inconsistency of the original van der Waals equation (3). Each molecule will have its own Janus van der Waals equation characterised by two input parameters, χ (continuous) and $n = 2, 4, 6$ (discrete).

With four constants $\{a, b, s, t\}$ which will be determined shortly, we require the spinodal curve to meet

$$T_r = -(v_r - b)^2 \frac{df_n(v_r)}{dv_r} = 1 - \frac{(v_r - a)^n (v_r - 1)^2 (v_r^2 - s v_r + t)}{v_r^{n+4}}. \quad (8)$$

While the first equality comes from the definition of the spinodal curve, crucially the second generalises the van der Waals case (5) and gives rise to two distinct critical points:

$$(n_c, P_r, T_r, v_r) = (n, 1 + \epsilon, 1, a) \quad \text{and} \quad (2, 1, 1, 1). \quad (9)$$

At each critical point, in view of (6), we have clearly

$$T_r - 1 \propto \begin{cases} (v_r - a)^n & \text{as } v_r \rightarrow a \\ (v_r - 1)^2 & \text{as } v_r \rightarrow 1 \end{cases}. \quad (10)$$

Their critical indices, pressure, and volume per particle may differ, but the critical temperature is the same, *i.e.* $T_r = 1$. For this, it is necessary to set $0 < a < 1$ and $s^2 \neq 4t$. We also put n to be even, $n = 0, 2, 4, 6, \dots$, such that the critical temperature is (locally) maximal on the spinodal curve, which is the case with the van der Waals fluid (5), a relativistic ideal Bose gas [8] (Figures 2 and 6 therein), and supposedly real molecules. Accordingly the spinodal curve (8) has ‘twin peaks’ in temperature, as depicted in **Figure 1**. Moreover, in order to be consistent with the realistic molecules for which only one critical point has been usually assumed, we shall let a be close to 1^- and then, from $\epsilon \propto (1 - a)^{n+3}$ which we shall derive later in (17), the two critical pressure, $P_r = 1$ and $P_r = 1 + \epsilon$, will be practically indistinguishable from each other.

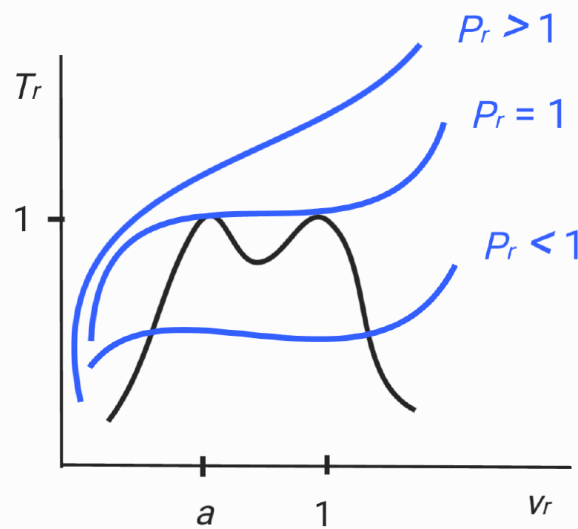


Figure 1. Schematic zoomed-in diagram of a spinodal curve (black colored) and three isobar curves (blue colored). There are two adjacent critical points on a spinodal curve at $v_r = a$ and at $v_r = 1$. When $P_r < 1$ the isobar crosses the spinodal curve twice at $v_r < a$ and at $v_r > 1$. When $P_r > 1$ the isobar does not meet the spinodal curve. When $P_r = 1$, with negligible ϵ , the critical isobar touches the spinodal curve at the two critical points. Specifically, along the critical isobar, as the temperature increases from $T_r < 1$ to $T_r = 1^-$, the critical point at $v_r = a$ with the critical index of $n_c = n = 2, 4, 6$ is relevant. On the other hand, as the temperature decreases from $T_r > 1$ to $T_r = 1^+$, the dominant critical point is at $v_r = 1$ with $n_c = 2$.

Between the two peaks on the spinodal curve, there is a local minimum which may be also identified as a ‘critical point’ of which the critical temperature is less than T_c . This third critical point is sandwiched by the two extremely adjacent critical points and plays little role in our analysis. The diagram generalises the single-peaked spinodal curve of a relativistic ideal Bose gas, depicted in **Figure 1 of Ref.[8]**, to twin-peaks, and furthermore will be confirmed through a concrete example as in **Figure 2**.

From the fact that the last expression in (8) should be divisible by $(v_r - b)^2$, two constraints arise:

$$(b - 1)^2(b - a)^n(b^2 - sb + t) = b^{n+4}, \quad \frac{2}{b-1} + \frac{n}{b-a} + \frac{2b-s}{b^2-sb+t} = \frac{n+4}{b}, \quad (11)$$

which subsequently determine s and t in terms of a and b ,

$$s = 2b + \left(\frac{(n+2)ab - (n+4)a + 4b - 2b^2}{(b-1)^3(b-a)^{n+1}} \right) b^{n+3}, \quad t = b^2 + \left(\frac{(n+1)ab - (n+3)a + 3b - b^2}{(b-1)^3(b-a)^{n+1}} \right) b^{n+4}. \quad (12)$$

With these identifications, the second equality of (8) fixes the function $f_n(v_r)$,

$$f_n(v_r) = \frac{1}{b^5} \sum_{l=0}^{n+1} \frac{c_l}{n+3-l} \left(\frac{b}{v_r} \right)^{n+3-l}, \quad (13)$$

where the coefficients are given, with (12), by²

$$c_l = \sum_{j=0}^l (j-l-1) \left[\binom{n}{j-4} a^4 + \binom{n}{j-3} (2+s)a^3 + \binom{n}{j-2} (1+2s+t)a^2 + \binom{n}{j-1} (s+2t)a + \binom{n}{j} t \right] \left(-\frac{a}{b} \right)^{n-j}. \quad (14)$$

Note that the binomial coefficient $\binom{n}{k} = \frac{n!}{k!(n-k)!}$ should be trivial if k or $n - k$ is negative.

The remaining two constants a, b are then determined by requiring that the reduced critical pressure P_r should take the aforementioned values of $1 + \epsilon$ and 1 at the two critical points of $v_r = a$ and $v_r = 1$ (9):

$$\chi \left[\frac{1}{a-b} - f_n(a) \right] = 1 + \epsilon, \quad \chi \left[\frac{1}{1-b} - f_n(1) \right] = 1. \quad (15)$$

We obtain from the latter

$$\chi = \frac{(n+3)(1-b)^{n+3}}{(1-b)^{n+3} + b^{n+3}}, \quad (16)$$

and subtracting the latter from the former

$$\epsilon = \frac{2\chi(1-a)^{n+3} \left[(1-b)^3(a-b)^{n+1} + \{(n+1)a - b + 3\} b^{n+3} \right]}{(n+3)(n+2)(n+1)a^3(1-b)^3(a-b)^{n+1}}. \quad (17)$$

Inverting (16), we solve for b in terms of the physically measurable compressibility factor,

$$b = \frac{(n+3-\chi)^{\frac{1}{n+3}}}{(n+3-\chi)^{\frac{1}{n+3}} + \chi^{\frac{1}{n+3}}}. \quad (18)$$

Clearly from (17), ϵ becomes small $\epsilon \propto (1-a)^{n+3}$ as the constant a gets close to unity from below. In fact, ϵ is positive when $0 < a < 1$ and $0 < \chi < n+3$. This confirms that the two critical points (9) can be indeed extremely adjacent and experimentally indistinguishable. Naturally, the limit $a \rightarrow 1^-$ does

² Essentially, the coefficients (14) stem from a recurrence relation $c_l - 2c_{l-1} + c_{l-2} = h_l$ for some h_l , whose solution reads in general $c_l = \sum_{j=0}^l (l+1-j)h_j$.

not match the exact value of $a = 1$: the former is still bi-critical while the latter is mono-critical with the enhanced critical index $n_c = n+2$. However, away from the critical points in the phase diagram, we may practically put

$$a \approx 1, \tag{19}$$

and obtain approximate Janus van der Waals equations which we shall test against NIST Reference Data [6].

Figure 2 is the diagram of a spinodal curve (8) for the choice of $n = 4$, $a = 0.99$, and $\chi = 3.4556$ as for nitrogen (N_2). It follows from (18) $b = 0.5009$ and subsequently (12) fixes s, t . The curve confirms the anticipated two adjacent critical points at $a = 0.99$ and 1.00 . Spinodal curves for other molecules can be obtained by the same method.

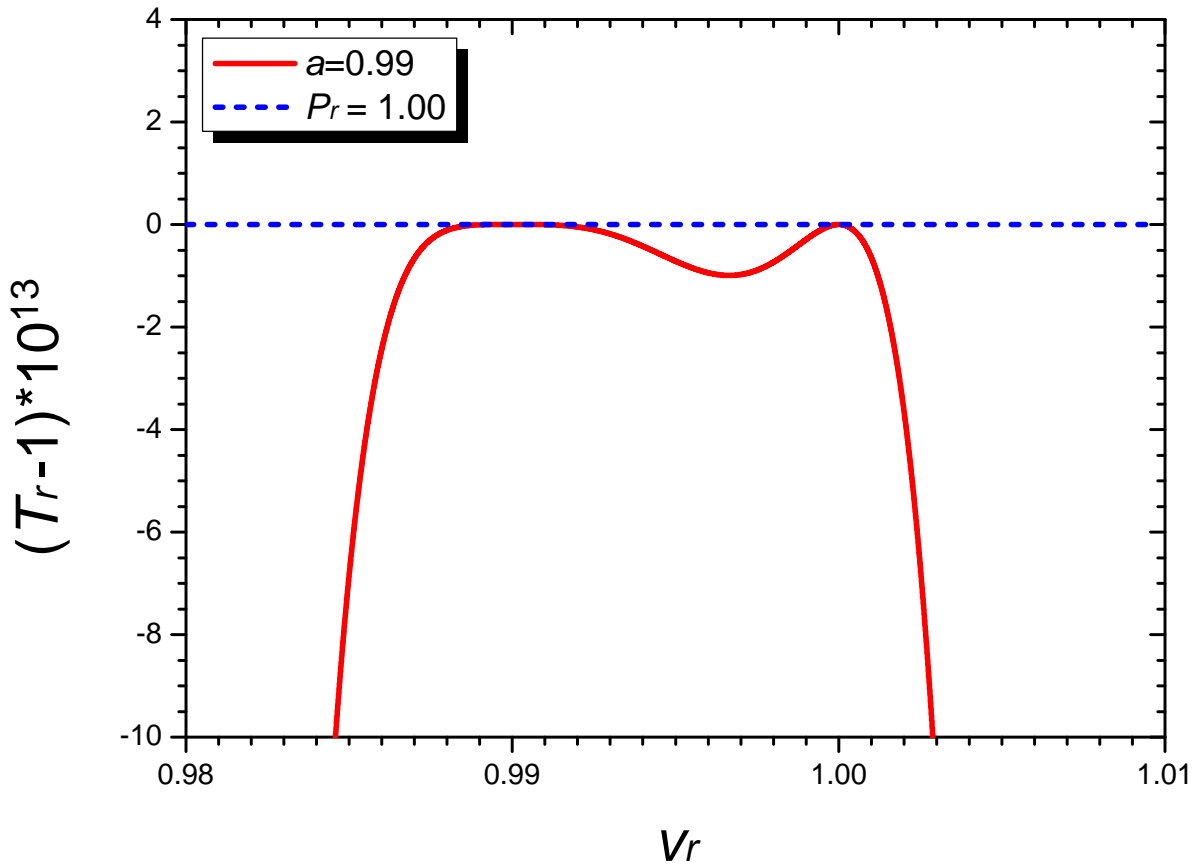


Figure 2. Diagram featuring the spinodal curve (red colored) and the critical isobar (blue colored) of the $n = 4$ Janus van der Waals equation with two adjacent critical points at $v_r = a = 0.99$ and $v_r = 1.00$. We have set $\chi = 3.4556$ as for nitrogen (N_2). Since $\epsilon = 6.0846 \times 10^{-15}$ (17), the two critical isobars, $P_r = 1$ and $P_r = 1 + \epsilon$, are indeed practically indistinguishable. The (common) critical isobar then touches both critical points, as anticipated in **Figure 1**. The local minimum value of T_r sandwiched by the twin critical points is lower than 1 by tiny small amount ($< 10^{-12}$), and thus also experimentally hard to detect.

3 THEORETICAL RESULT: JANUS VAN DER WAALS EQUATIONS

We now spell our modified van der Waals equations for each case of $n = 0$ (mono-critical) and $n = 2, 4$ (bi-critical/Janus) explicitly.

3.1 $n = 0$: mono-critical generalisation

When $n = 0$, the parameter a becomes irrelevant as there is only one critical point. Consequently, (7) reduces to an one-parameter generalisation of the van der Waals equation,

$$\left[P_r + \frac{\left[\chi^{\frac{1}{3}} - (\chi - 3)^{\frac{1}{3}} \right] \left[\chi^{\frac{2}{3}} - |\chi - 3|^{\frac{2}{3}} \right]}{v_r^2} + \frac{2 - \chi + \chi^{\frac{1}{3}} |\chi - 3|^{\frac{2}{3}}}{v_r^3} \right] \left[v_r - \frac{(\chi - 3)^{\frac{1}{3}}}{(\chi - 3)^{\frac{1}{3}} - \chi^{\frac{1}{3}}} \right] = \chi T_r. \quad (20)$$

The critical compressibility factor is at our disposal. Choosing $\chi = \frac{k_B T_c}{P_c v_c} = \frac{8}{3}$, one recovers the original van der Waals equation (1).

Among the eleven major molecules we examine, cyclopentane is exceptional, as its critical phase transition is not two-sided: $n_c = 2$ universally for the temperature $T > T_c$ and $T < T_c$ [5]. Logically, it can be either mono-critical with $n = 0$ or bi-critical with $n = 2$. To examine which is correct with the NIST data, we put $\chi = 3.5572$ as for the value of cyclopentane, and prepare an $n = 0$ equation from (20),

$$\left(P_r + \frac{1.1632}{v_r^2} - \frac{0.52356}{v_r^3} \right) (v_r + 1.1694) = 3.5572 T_r. \quad (21)$$

The plus sign in the second bracket (which is generically the case for $\chi > 3$) contrasts with the negative sign in the original van der Waals equation (1).

3.2 $n = 2$ equation for cyclopentane (C_5H_{10})

For $n = 2$, in the limit $a \rightarrow 1^-$ or $a \approx 1$ (19), we have

$$\begin{aligned} \chi f_{n=2}(v_r) \approx & \frac{\chi^{\frac{1}{5}}(5-\chi)^{\frac{1}{5}} \left[\chi^{\frac{1}{5}} - (5-\chi)^{\frac{1}{5}} \right] \left[\chi^{\frac{2}{5}} + (5-\chi)^{\frac{2}{5}} \right] + 4\chi - 10}{v_r^2} + \frac{\chi^{\frac{1}{5}}(5-\chi)^{\frac{2}{5}} \left[\chi^{\frac{2}{5}} - 2\chi^{\frac{1}{5}}(5-\chi)^{\frac{1}{5}} + 3(5-\chi)^{\frac{2}{5}} \right] - 6\chi + 20}{v_r^3} \\ & + \frac{\chi^{\frac{1}{5}}(5-\chi)^{\frac{3}{5}} \left[\chi^{\frac{1}{5}} - 3(5-\chi)^{\frac{1}{5}} \right] + 4\chi - 15}{v_r^4} + \frac{\chi^{\frac{1}{5}}(5-\chi)^{\frac{4}{5}} - \chi + 4}{v_r^5}. \end{aligned} \quad (22)$$

Letting $\chi = 3.5572$, we obtain an $n = 2$ Janus van der Waals equation for C_5H_{10} (cyclopentane),

$$\left(P_r + \frac{5.0608}{v_r^2} + \frac{2.1811}{v_r^3} - \frac{3.8860}{v_r^4} + \frac{2.1710}{v_r^5} \right) (v_r - 0.45500) \approx 3.5572 T_r. \quad (23)$$

As we shall see in the next section, the NIST data of cyclopentane is better described by this bi-critical equation rather than the mono-critical one (21).

3.3 $n = 4$ equations for nitrogen (N_2), argon (Ar), methane (CH_4), ethylene (C_2H_4), ethane (C_2H_6), propylene (C_3H_6), propane (C_3H_8), butane (C_4H_{10}), and isobutane (C_4H_{10})

For $n = 4$ with $b = \frac{(7-\chi)^{\frac{1}{7}}}{(7-\chi)^{\frac{1}{7}} + \chi^{\frac{1}{7}}}$ and $a \approx 1$ (19), we have

$$\begin{aligned} \chi f_{n=4}(v_r) \approx & \frac{21-140b+392b^2-588b^3+490b^4-196b^5}{[b^7+(1-b)^7]v_r^2} + \frac{-35+245b-728b^2+1176b^3-1078b^4+490b^5}{[b^7+(1-b)^7]v_r^3} \\ & + \frac{35-245b+735b^2-1218b^3+1176b^4-588b^5}{[b^7+(1-b)^7]v_r^4} + \frac{-21+147b-441b^2+735b^3-728b^4+392b^5}{[b^7+(1-b)^7]v_r^5} \\ & + \frac{7-49b+147b^2-245b^3+245b^4-140b^5}{[b^7+(1-b)^7]v_r^6} + \frac{-1+7b-21b^2+35b^3-35b^4+21b^5}{[b^7+(1-b)^7]v_r^7}. \end{aligned} \quad (24)$$

Choosing χ from experimental data, we obtain $n = 4$ Janus van der Waals equations for nine molecules,

$$\left(P_r + \frac{k_2}{v_r^2} + \frac{k_3}{v_r^3} + \frac{k_4}{v_r^4} + \frac{k_5}{v_r^5} + \frac{k_6}{v_r^6} + \frac{k_7}{v_r^7} \right) (v_r - b) \approx \chi T_r, \quad (25)$$

of which the coefficients are listed in **Table 1**.

molecule ($n = 4$)	χ	k_2	k_3	k_4	k_5	k_6	k_7	b
nitrogen (N_2)	3.4556	-0.30474	28.762	-57.117	56.913	-28.406	6.0760	0.50091
argon (Ar)	3.4542	-0.31380	28.784	-57.150	56.941	-28.418	6.0783	0.50093
methane (CH_4)	3.4936	-0.044104	28.110	-56.162	56.132	-28.059	6.0110	0.50013
ethylene (C_2H_4)	3.5563	0.38638	27.034	-54.582	54.840	-27.484	5.9032	0.49885
ethane (C_2H_6)	3.5726	0.49759	26.755	-54.174	54.505	-27.335	5.8752	0.49852
propylene (C_3H_6)	3.6279	0.87670	25.806	-52.781	53.364	-26.827	5.7797	0.49739
propane (C_3H_8)	3.6168	0.80075	25.996	-53.060	53.593	-26.929	5.7989	0.49762
butane (C_4H_{10})	3.6529	1.0482	25.376	-52.150	52.847	-26.597	5.7363	0.49688
isobutane (C_4H_{10})	3.6251	0.85816	25.852	-52.849	53.420	-26.852	5.7844	0.49744

Table 1. The coefficients of the $n = 4$ Janus van der Waals equations for nine molecules.

3.4 $n = 6$ equation for helium-4 (^4He)

For $n = 6$ with $b = \frac{(9-\chi)^{\frac{1}{9}}}{(9-\chi)^{\frac{1}{9}} + \chi^{\frac{1}{9}}}$ and $a \approx 1$ (19), we have

$$\begin{aligned} \chi f_{n=6}(v_r) \approx & \frac{36-315b+1215b^2-2700b^3+3780b^4-3402b^5+1890b^6-540b^7}{[b^9+(1-b)^9]v_r^2} \\ & + \frac{-84+756b-3015b^2+6975b^3-10260b^4+9828b^5-5922b^6+1890b^7}{[b^9+(1-b)^9]v_r^3} \\ & + \frac{126-1134b+4536b^2-10575b^3+15795b^4-15552b^5+9828b^6-3402b^7}{[b^9+(1-b)^9]v_r^4} \\ & + \frac{-126+1134b-4536b^2+10584b^3-15867b^4+15795b^5-10260b^6+3780b^7}{[b^9+(1-b)^9]v_r^5} \\ & + \frac{84-756b+3024b^2-7056b^3+10584b^4-10575b^5+6975b^6-2700b^7}{[b^9+(1-b)^9]v_r^6} \\ & + \frac{-36+324b-1296b^2+3024b^3-4536b^4+4536b^5-3015b^6+1215b^7}{[b^9+(1-b)^9]v_r^7} \\ & + \frac{9-81b+324b^2-756b^3+1134b^4-1134b^5+756b^6-315b^7}{[b^9+(1-b)^9]v_r^8} \\ & + \frac{-1+9b-36b^2+84b^3-126b^4+126b^5-84b^6+36b^7}{[b^9+(1-b)^9]v_r^9}. \end{aligned} \quad (26)$$

Letting $\chi = 3.2991$, we get an $n = 6$ Janus van der Waals equation for helium-4,

$$\left(P_r - \frac{10.671}{v_r^2} + \frac{97.188}{v_r^3} - \frac{259.53}{v_r^4} + \frac{393.69}{v_r^5} - \frac{366.57}{v_r^6} + \frac{210.75}{v_r^7} - \frac{69.112}{v_r^8} + \frac{10.066}{v_r^9} \right) (v_r - 0.51519) \approx 3.2991 T_r. \quad (27)$$

4 COMPARISON WITH NIST REFERENCE DATA

Henceforth we look into isochoric, isobaric and isothermal cases for real molecules, which will demonstrate that our Janus van der Waals equations represent excellent agreements with the NIST data, better than the original van der Waals equation. By construction, the Janus van der Waals equations reflect the previously reported two-sided critical phenomena [5] and at the same time reduce consistently to the classical ideal gas law in the low density limit far away from the critical point at $v_r = 1$.

First, we focus on the $n = 2$ case which only cyclopentane molecule (C_5H_{10}) belongs to.

Figure 3 shows the isochoric curves of cyclopentane molecule at $1/v_r = 0.02$ (**A**), $1/v_r = 0.5$ (**B**), $1/v_r = 1.0$ (**C**), and $1/v_r = 1.5$ (**D**) respectively. They are drawn by the NIST data and further by the four equations: the $n = 2$ Janus van der Waals equation (23), the mono-critical equation ($n = 0$) (21), the original van der Waals equation (1), and the classical ideal gas law (2). The $n = 2$ Janus van der Waals equation fits best with the NIST data, while consistently reducing to the classical ideal gas law in low

density limit.

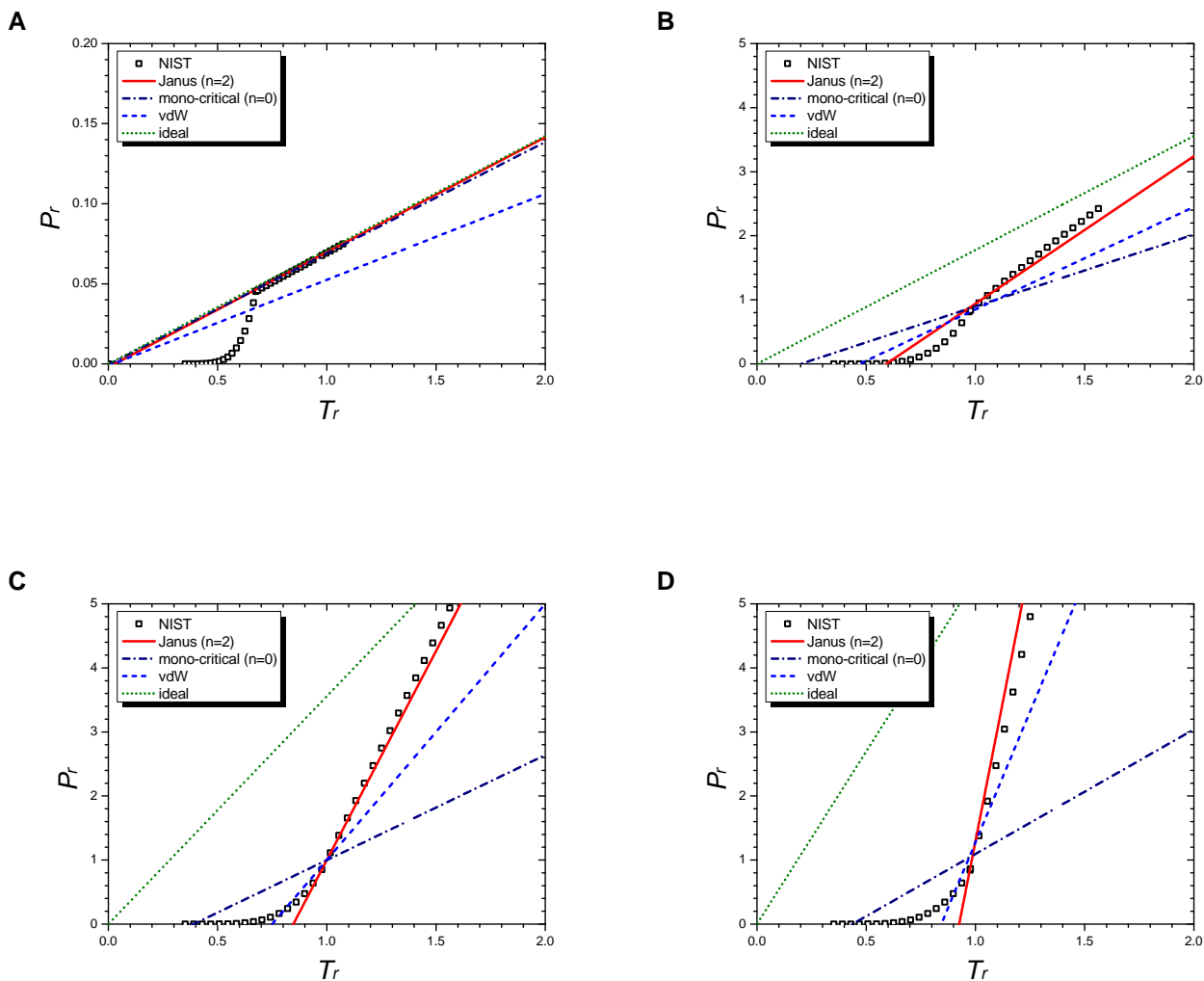


Figure 3. Isochoric curves of cyclopentane (C_5H_{10}) at $1/v_r = 0.02$ (**A**), $1/v_r = 0.5$ (**B**), $1/v_r = 1.0$ (**C**), and $1/v_r = 1.5$ (**D**). Boxes are from the NIST data. The red solid line is drawn from the $n = 2$ Janus van der Waals equation (23) and is better fitted than the three others: the $n = 0$ mono-critical equation (21), the original van der Waals equation (1), and the classical ideal gas law (2).

Figure 4 shows the isobaric curves of cyclopentane molecule (C_5H_{10}) at $P_r = 1.5$ (**A**), $P_r = 1.0$ (**B**), and $P_r = 0.5$ (**C**) respectively. They are drawn by the NIST data and further by the four equations: the $n = 2$ Janus van der Waals equation (23), the mono-critical equation ($n = 0$) (21), the original van der Waals equation (1), and the classical ideal gas law (2). The $n = 2$ Janus van der Waals equation is in excellent agreement with the NIST data, especially at the liquid-vapor coexistence region near $P_r = 1$ as well as at the supercritical region of $P_r > 1$.

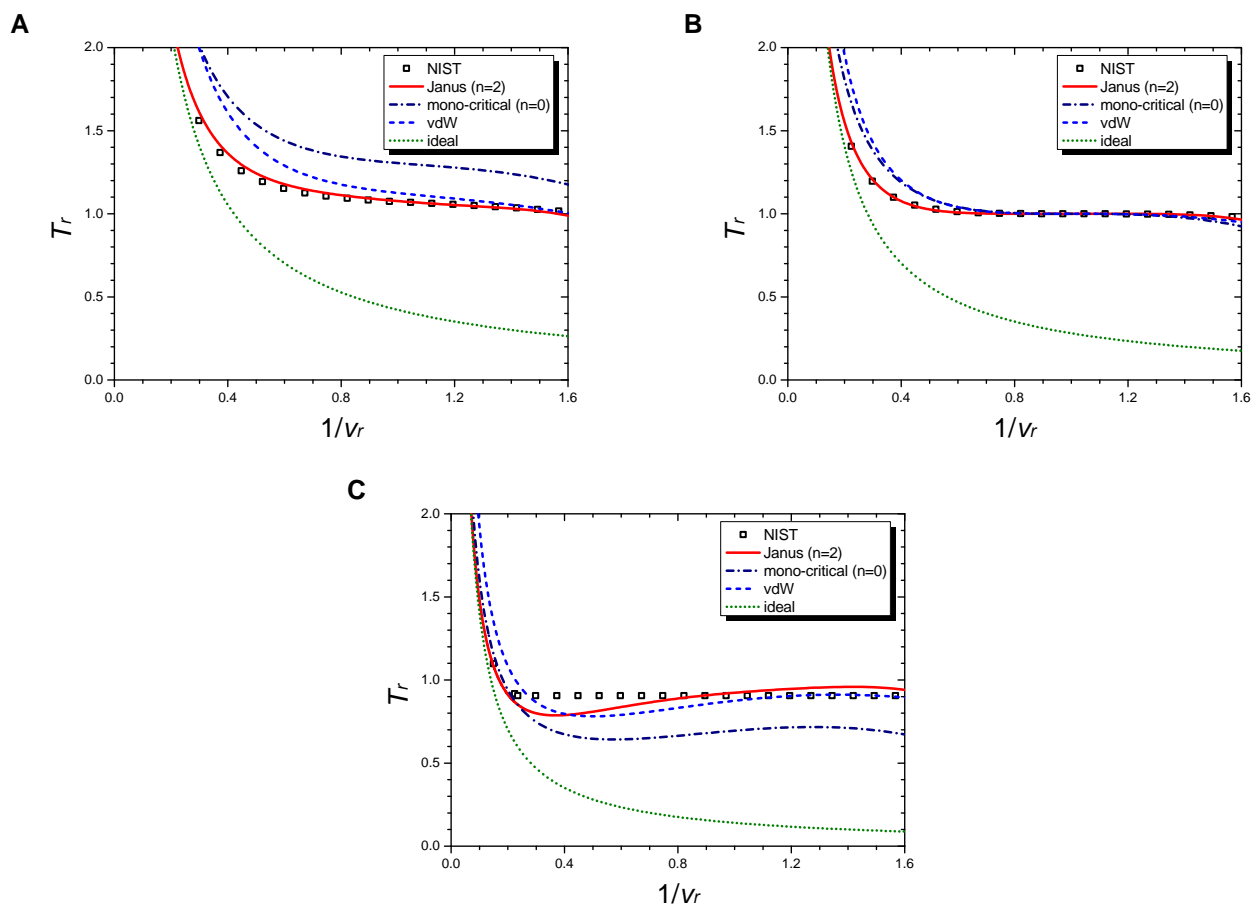


Figure 4. Isobaric curves of cyclopentane (C_5H_{10}) at $P_r = 1.5$ (**A**), $P_r = 1.0$ (**B**), and $P_r = 0.5$ (**C**). Boxes are from the NIST data. The red solid line is drawn from the $n = 2$ Janus van der Waals equation (23) and is better fitted than the $n = 0$ mono-critical equation (21), the original van der Waals equation (1), or the classical ideal gas law (2).

Figure 5 shows the isothermal curves of cyclopentane molecule (C_5H_{10}) at $T_r = 1.01$ (**A**), $T_r = 1.00$ (**B**), and $T_r = 0.99$ (**C**) respectively. They are drawn by the NIST data and further by the four equations: the $n = 2$ Janus van der Waals equation (23), the mono-critical equation ($n = 0$) (21), the original van der Waals equation (1), and the classical ideal gas law (2). The Janus van der Waals equation shows enhanced sigmoid shape compared to the original van der Waals equation when T_r is lower than 1.

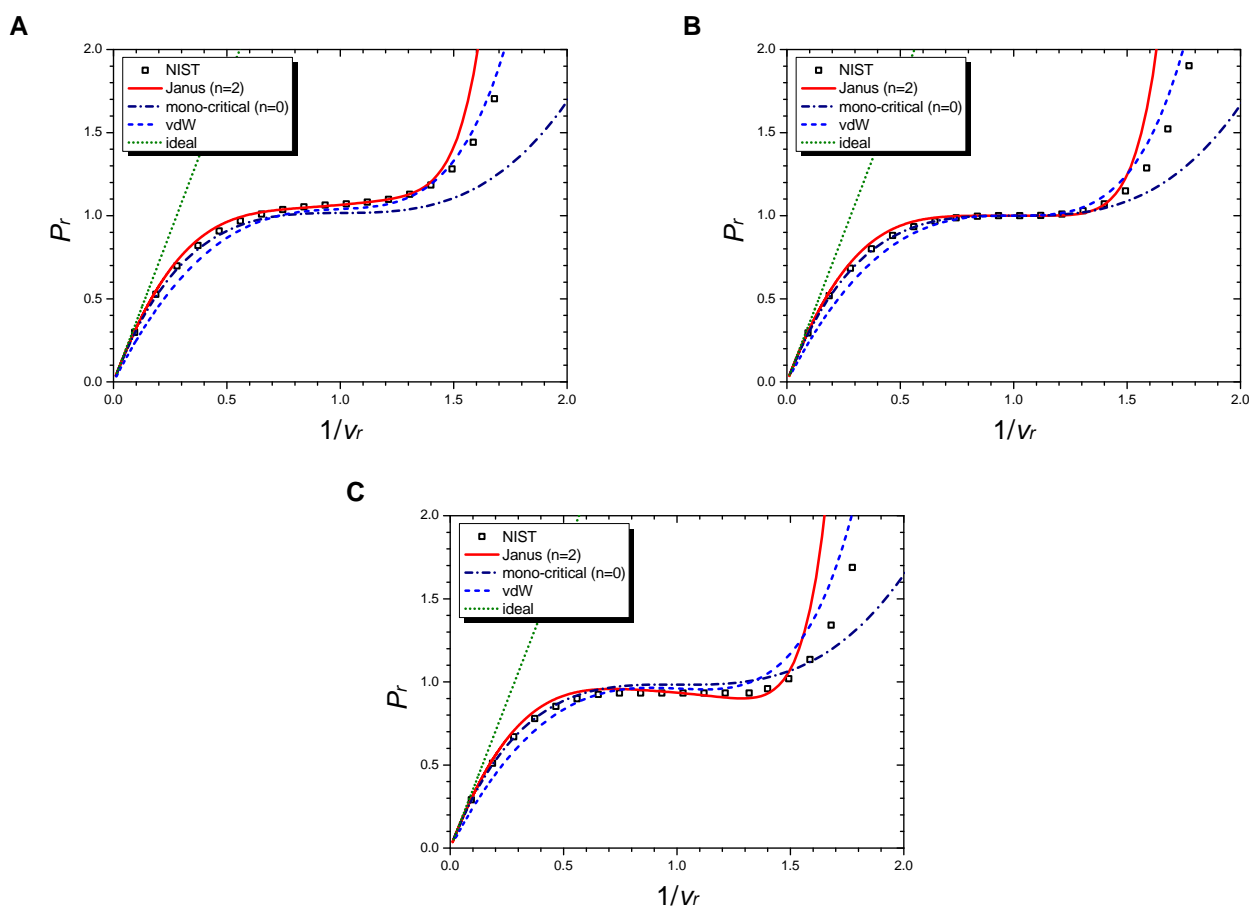


Figure 5. Isothermal curves of cyclopentane (C_5H_{10}) at $T_r = 1.01$ (**A**), $T_r = 1.00$ (**B**), and $T_r = 0.99$ (**C**). Boxes are from the NIST data. The red solid line is drawn from the $n = 2$ Janus van der Waals equation (23) and is better fitted than the $n = 0$ mono-critical equation (21), the original van der Waals equation (1), or the classical ideal gas law (2).

Figure 6 shows the three-dimensional $P_r - v_r - T_r$ phase diagram of the exact $n = 2$ Janus van der Waals equation (7) with (13), as for cyclopentane molecule (C_5H_{10}). The red line shows the spinodal curve (8), *i.e.* $\partial_v P(T, v) = 0$, of the Janus van der Waals equation with the choice of $a = 0.99$.

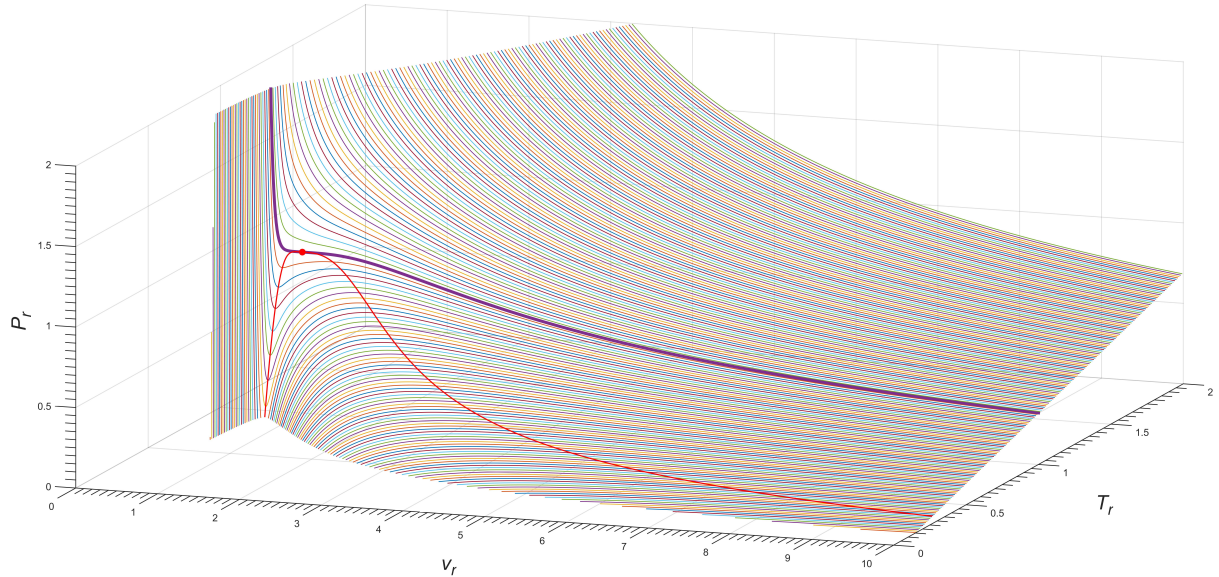


Figure 6. Three-dimensional $P_r - v_r - T_r$ phase diagram of the exact $n = 2$ Janus van der Waals equation (7), as for cyclopentane molecule (C_5H_{10}). The bold purple line corresponds to the isotherm of $T_r = 1.00$ as depicted in **Figure 5 B**; the red line is the Janus van der Waals spinodal curve with $a = 0.99$; and the red dot is the critical point.

Now, we turn to the case of $n = 4$ which the following nine molecules belong to: nitrogen (N_2), argon (Ar), methane (CH_4), ethylene (C_2H_4), ethane (C_2H_6), propylene (C_3H_6), propane (C_3H_8), butane (C_4H_{10}), and isobutane (C_4H_{10}). Here we choose nitrogen as a representative example. The other eight molecules as well as the $n = 6$ case which only helium-4 molecule belongs to are dealt in the Supplementary Material separately.

Figure 7 shows the isochoric curves of nitrogen (N_2) at $1/v_r = 0.02$ (**A**), $1/v_r = 0.5$ (**B**), $1/v_r = 1.0$ (**C**), and $1/v_r = 1.5$ (**D**) respectively. They are drawn by the NIST data and further by the four equations: the Janus van der Waals equation for $n = 4$ (25), the original van der Waals equation (1), and the classical ideal gas law (2). The Janus van der Waals equation fits best with the NIST data, especially at the region of $T_r > 1$ better than the original van der Waals equation. Again, we confirm that the $n = 4$ Janus van der Waals equation reduces to the classical ideal gas law in low density limit.

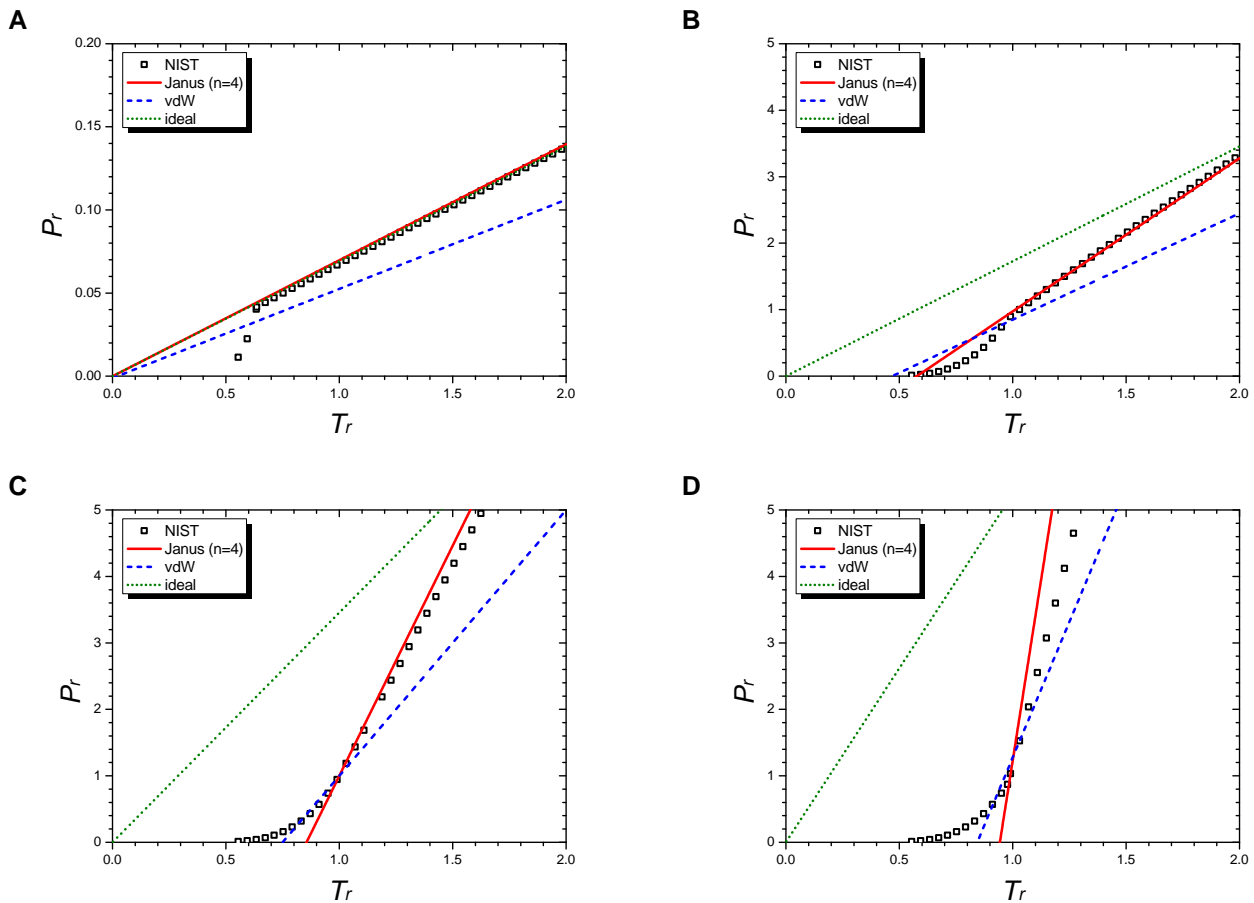


Figure 7. Isochoric curves of nitrogen (N_2) at $1/v_r = 0.02$ (**A**), $1/v_r = 0.5$ (**B**), $1/v_r = 1.0$ (**C**), and $1/v_r = 1.5$ (**D**). Boxes are from the NIST data. The red solid line is drawn from the $n = 2$ Janus van der Waals equation (23) and is better fitted than the original van der Waals equation (1) or the classical ideal gas law (2).

Figure 8 shows the isobaric curves of nitrogen (N_2) at $P_r = 1.5$ (**A**), $P_r = 1.0$ (**B**), and $P_r = 0.5$ (**C**) respectively. They are drawn by the NIST data and further by the three equations: the Janus van der Waals equation for $n = 4$ (25), the original van der Waals equation (1), and the classical ideal gas law (2). The $n = 4$ Janus van der Waals equation is in excellent agreement with the NIST data, especially at the liquid-vapor coexistence region near $P_r = 1$ as well as at the supercritical region of $P_r > 1$.

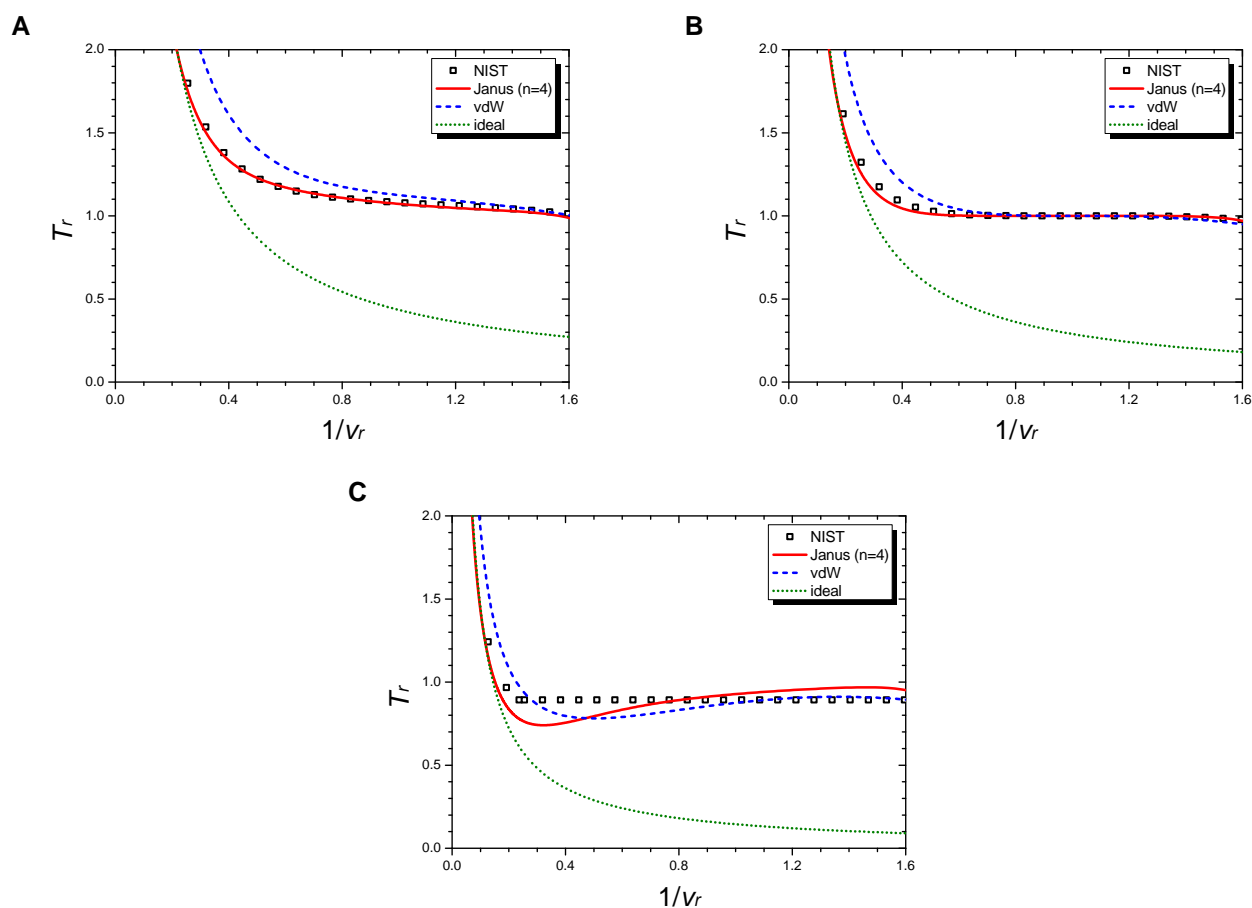


Figure 8. Isobaric curves of nitrogen (N_2) at $P_r = 1.5$ (**A**), $P_r = 1.0$ (**B**), and $P_r = 0.5$ (**C**). Boxes are from the NIST data. The red solid line is drawn from the $n = 4$ Janus van der Waals equation (25) and is better fitted than the original van der Waals equation (1) or the classical ideal gas law (2).

Figure 9 shows the isothermal curves of nitrogen (N_2) at $T_r = 1.01$ (**A**), $T_r = 1.00$ (**B**), and $T_r = 0.99$ (**C**) respectively. They are drawn by the NIST data and further by the three equations: the $n = 4$ Janus van der Waals equation (25), the original van der Waals equation (1), and the classical ideal gas law (2). The Janus van der Waals equation shows enhanced sigmoid shape compared to the original van der Waals equation when T_r is lower than 1.

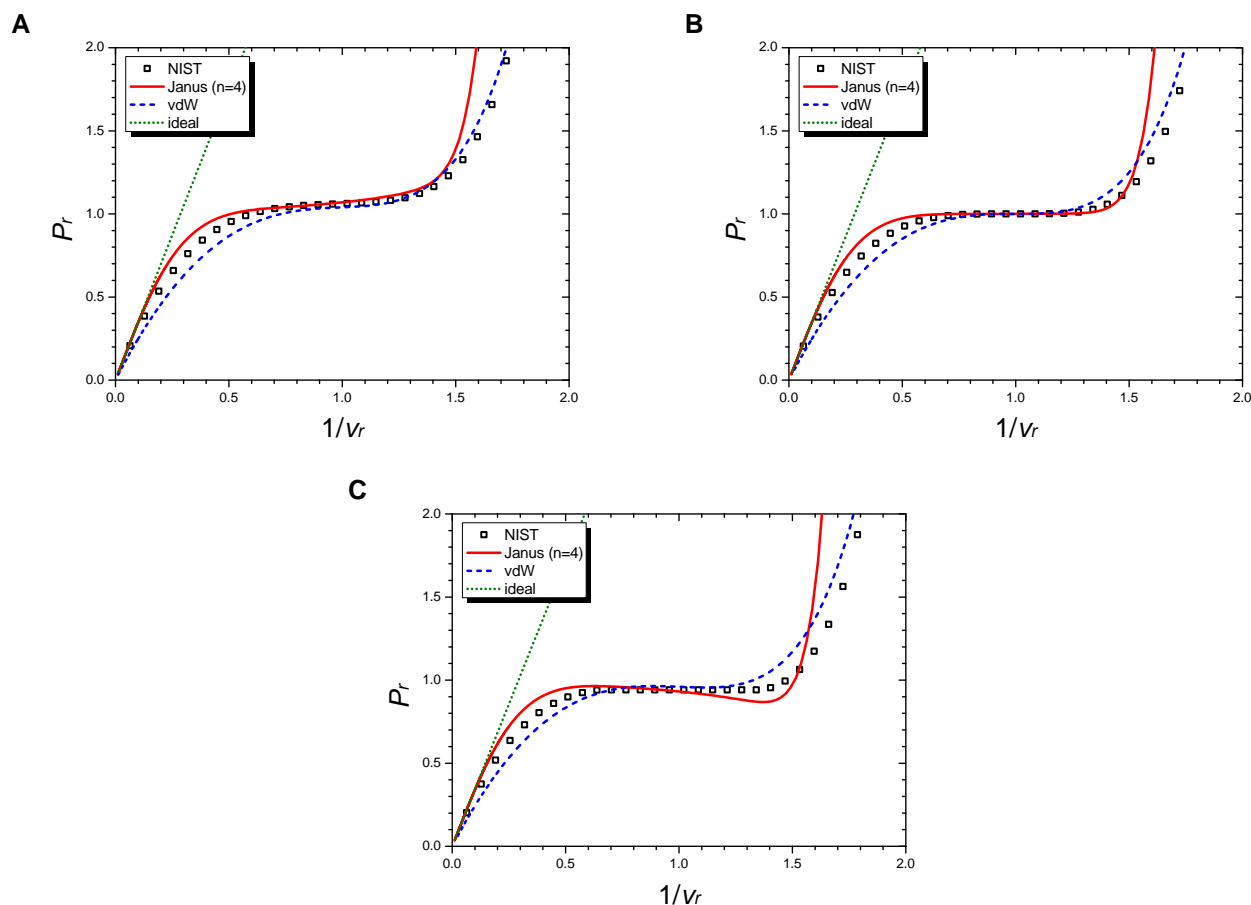


Figure 9. Isothermal curves of nitrogen (N_2) at $T_r = 1.01$ (**A**), $T_r = 1.00$ (**B**), and $T_r = 0.99$ (**C**). Boxes are from the NIST data. The red solid line is drawn from the $n = 4$ Janus van der Waals equation (25) and is better fitted than the original van der Waals equation (1) or the classical ideal gas law (2).

Figure 10 shows the three-dimensional $P_r - v_r - T_r$ phase diagram of the exact $n = 4$ Janus van der Waals equation (7) with (13), as for nitrogen (N_2). The red line shows the spinodal curve (8), *i.e.* $\partial_v P(T, v) = 0$, of the Janus van der Waals equation with the choice of $a = 0.99$.

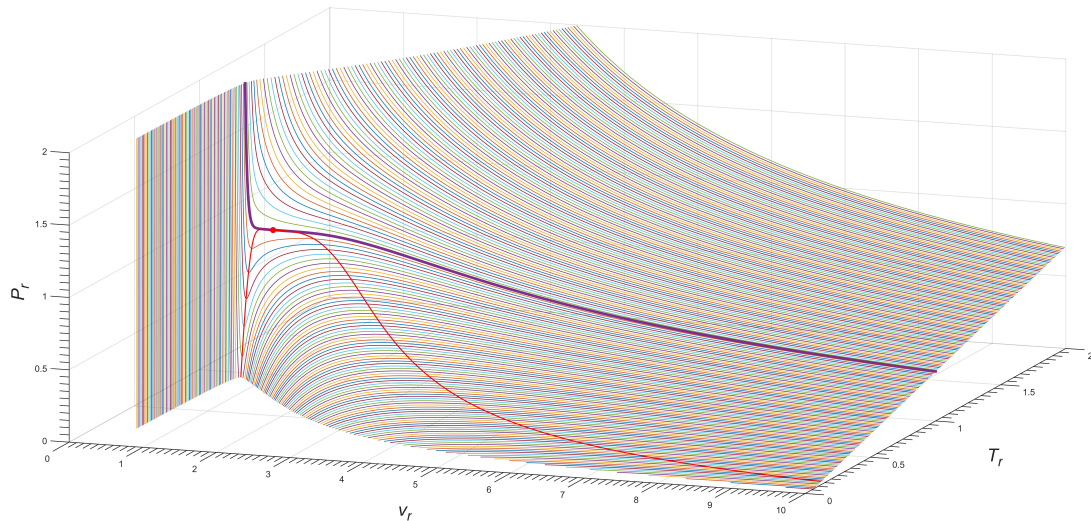


Figure 10. Three-dimensional $P_r - v_r - T_r$ phase diagram of the exact $n = 4$ Janus van der Waals equation (7), as for nitrogen (N_2). The bold purple line corresponds to the isotherm of $T_r = 1.00$ as depicted in **Figure 9 B**; the red line is the Janus van der Waals spinodal curve with $a = 0.99$; and the red dot is the critical point.

5 DISCUSSION

Our Janus van der Waals equations may appear somewhat similar to other known equations of state, such as the virial equation of state, a typical example of series expansion [9]. Irrespective of the similarity of appearance to other equations, the Janus van der Waals equations differ totally from others, as the starting point is directly from statistical physics itself at quantum level: namely that the partition function of any finite system should be analytic. Alternative to the conventional thermodynamic limit [10, 11], if we persistently take the analyticity of a partition function for granted [12, 8, 13, 14, 15], it becomes the spinodal curve itself that draws the liquid-gas phase diagram where a critical point is identified as the extremum of the spinodal curve, see [8] and Figure 6 therein. One surprising result of the previous work by two of us [5] was the possibility of having P_c more than one critical points which should be very close to each other. Our ansatz (8) modifies the original van der Waals equation and realises the idea of multi-critical points in a simple manner, restricted to even critical indices, $n_c = n = 2, 4, 6$ for $T < T_c$ and $n_c = 2$ for $T > T_c$, or following the notation of [5], $(n_+, n_-) = (2, n)$. Our proposed van der Waals equations then naturally explain the two-sided phase transitions reported in [5] and provide overall effective descriptions of real molecules, in particular better than the original van der Waals equation as well as the classical ideal gas law.

In **Figure 11**, we have compared the NIST co-existence curve data of cyclopentane molecule (C_5H_{10}) with the Janus van der Waals spinodal curve (8) of $n = 2$, $a = 0.99$ and also with the original van der Waals spinodal curve (5). The Janus van der Waals spinodal curve fits well the NIST co-existence curve

data in a wider range near the critical point, though not perfect. Further modifications of the present Janus van der Waals equations to match the spinodal curves with the co-existence curves of real molecules will lead to more realistic, improved equations of state. Such modifications may require more than two critical points, generalising the ansatz (8):

$$T_r = -(v_r - b)^2 \frac{df_{\vec{n}}(v_r)}{dv_r} = 1 - \prod_{i=1}^N \frac{(v_r - a_i)^{n_i}}{v_r}. \quad (28)$$

Here n_i 's are natural numbers, and especially those a_i 's with $n_i \geq 2$ (even as well as odd) correspond to multi-critical points. The largest value of such a_i 's should be exactly unity with the critical index 2 as the NIST data suggests [5], while the smallest one should be still close to unity. Further, the former should be a local maximum of T_r , while the latter should be either a local maximum as in **Figure 1** if the critical index is even or an inflection point if it is odd. We leave the construction of this kind of multi-critical Janus van der Waals equations for future work.

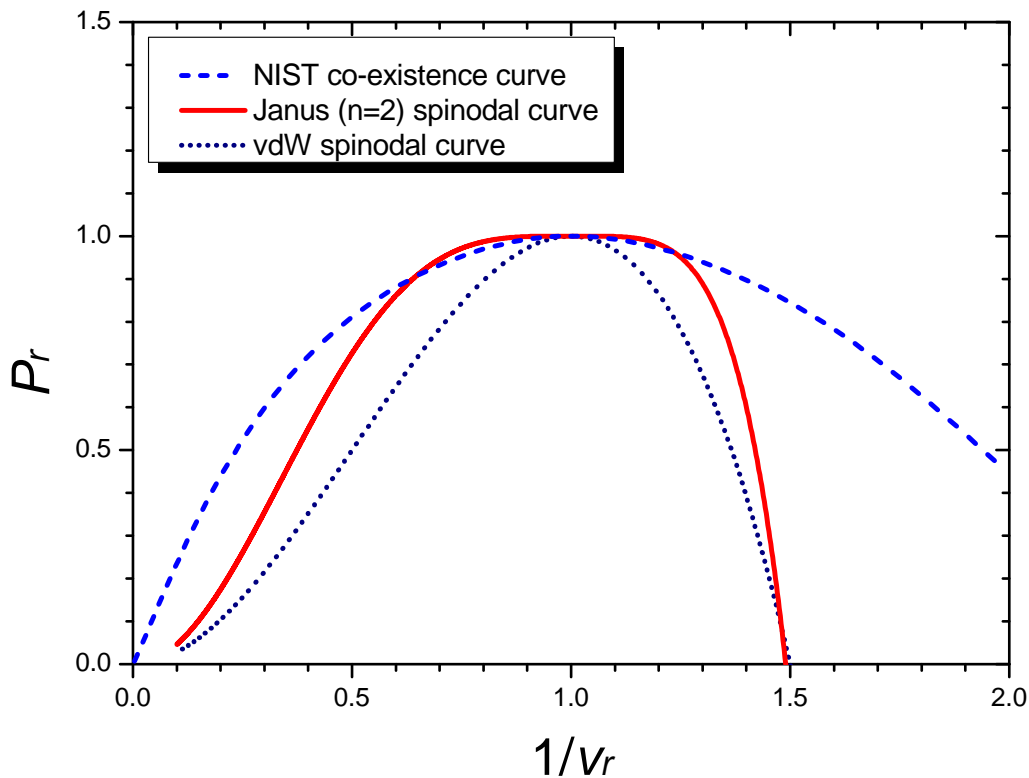


Figure 11. Comparison of the NIST co-existence curve data of cyclopentane (C_5H_{10}) (blue colored) with the Janus van der Waals spinodal curve (red colored, $a = 0.99$) as well as with the original van der Waals spinodal curve (dotted black line). It is a conjecture of Ref.[8] that the liquid-gas co-existence curve should actually coincide with the spinodal curve. Improving our proposed Janus van der Waals equations further, this may be realisable.

The three Janus van der Waals equations (23), (25), (27) have been obtained after taking the limit $a \rightarrow 1^-$. Thus, the formulas should not be used to see the two-sided critical phase transitions for which the exact formula (7) with (13) must be taken and zoomed in sufficiently. When zoomed out, or moderately away from the two critical points, the two powers, $(v_r - a)^n$ and $(v_r - 1)^2$ in (8), may appear converging to $(v_r - 1)^{n+2}$ and mimic an enhanced critical index $n_c = n + 2$. This implies the critical exponents $\alpha_P = \gamma_P = \frac{n+2}{n+3}$, $\beta_P = \delta^{-1} = \frac{1}{n+3}$ and also explains the ‘flatness’ of the top of the spinodal curve in **Figure 11**. The three formulas (23), (25), (27) are for such effective descriptions. The NIST data analyses of [5], in particular the figures 2,3,4 therein, seem to agree with this enhancement moderately away from the critical points.

Having the Janus van der Waals equations completely determined, it is worth while to recall

$$P_r = \chi T_r \frac{\partial \ln Z(T_r, v_r)}{\partial v_r}, \quad (29)$$

and to obtain the underlying partition function (per particle),

$$\ln Z = \ln \left[(v_r - b) T_r^{3/2} \right] + \sum_{l=0}^{n+1} \frac{c_l (b/v_r)^{n+2-l}}{(n+3-l)(n+2-l)b^4 T_r}, \quad (30)$$

where the constant of integration $\frac{3}{2} \ln T_r$ has been added to ensure the isochoric specific heat $c_v = \frac{3}{2} k_B$ at high temperature.

Given the good agreement of the Janus van der Waals equations and the NIST Reference Data, which we report in this work, we call for further investigation of the multi-critical points and the analyticity of partition functions questioning the (rather dogmatic) thermodynamic limit.

CONFLICT OF INTEREST STATEMENT

The authors declare that the research was conducted in the absence of any commercial or financial relationships that could be construed as a potential conflict of interest.

AUTHOR CONTRIBUTIONS

J-HP proposed the research and derived the formulas. JK contributed the NIST Reference Data handling and analysis. D-HK led the interpretation of the data. D-HK and J-HP wrote the manuscript.

FUNDING

This work was supported by Basic Science Research Program through the National Research Foundation of Korea Grants, NRF-2016R1D1A1B01015196 and NRF-2020R1A6A1A03047877 (Center for Quantum Space Time).

ACKNOWLEDGMENT

We thank KyuHwan Lee for technical help at the early stage of the project.

SUPPLEMENTAL DATA

Figures of the eight molecules belonging to the $n = 4$ case and of helium-4 of the $n = 6$ case are included in the Supplementary Material (attached after References).

DATA AVAILABILITY STATEMENT

The datasets for this study is *NIST Reference Fluid Thermodynamic and Transport Properties Database (REFPROP): Version 9.1, National Institute of Standards and Technology (NIST), Standard Reference Data Program, Gaithersburg* and can be found at <https://www.nist.gov/srd/refprop> [6].

REFERENCES

- [1] J. Zinn-Justin, *Quantum Field Theory and Critical Phenomena*, 2nd ed. (Oxford University Press, New York, 1993), p. 610.
- [2] D. R. Nelson, “Coexistence-curve singularities in isotropic ferromagnets,” *Phys. Rev. B* **13**, 2222 (1976).
- [3] F. Léonard and B. Delamotte, “Critical Exponents Can Be Different on the Two Sides of a Transition: A Generic Mechanism,” *Phys. Rev. Lett.* **115** (2015) no.20, 200601 doi:10.1103/PhysRevLett.115.200601 [arXiv:1508.07852 [cond-mat.stat-mech]].
- [4] T. Azeyanagi, F. Ferrari and F. I. Schaposnik Massolo, “Phase Diagram of Planar Matrix Quantum Mechanics, Tensor, and Sachdev-Ye-Kitaev Models,” *Phys. Rev. Lett.* **120** (2018) no.6, 061602 doi:10.1103/PhysRevLett.120.061602 [arXiv:1707.03431 [hep-th]].
- [5] W. Cho, D.-H. Kim and J.-H. Park, “Isobaric Critical Exponents: Test of Analyticity against NIST Reference Data,” *Front. Phys.* **6** (2018) 112 doi:10.3389/fphy.2018.00112 [arXiv:1612.06532 [cond-mat.stat-mech]].
- [6] Lemmon EW, Huber ML, McLinden MO. 2013 NIST Reference Fluid Thermodynamic and Transport Properties Database (REFPROP): Version 9.1, National Institute of Standards and Technology (NIST), Standard Reference Data Program, Gaithersburg (<https://www.nist.gov/srd/refprop>).
- [7] D. Bak, M. Gutperle and S. Hirano, “A Dilatonic deformation of AdS(5) and its field theory dual,” *JHEP* **0305** (2003) 072 doi:10.1088/1126-6708/2003/05/072 [hep-th/0304129].
- [8] J.-H. Park and S.-W. Kim, “Existence of a critical point in the phase diagram of ideal relativistic neutral Bose gas,” *New J. Phys.* **13** 033003 (2011).
- [9] J.D. Dymond, K.N. Marsh, and R.C. Wilhoit, *Virial coefficients of pure gases and mixtures*, Springer Berlin Heidelberg (2003).
- [10] C. N. Yang and T. D. Lee, “Statistical Theory of Equations of State and Phase Transitions. I. Theory of Condensation,” *Phys. Rev.* **87** 404 (1952); “Statistical Theory of Equations of State and Phase Transitions. II. Lattice Gas and Ising Model,” *Phys. Rev.* **87** 410 (1952).
- [11] L. P. Kadanoff, “More is the Same; Phase Transitions and Mean Field Theories,” *J. Stat. Phys.* **137**, 777 (2009).
- [12] J.-H. Park and S.-W. Kim, “Thermodynamic instability and first-order phase transition in an ideal Bose gas,” *Phys. Rev. A* **81** 063636 (2010).
- [13] I. Jeon, S.-W. Kim and J.-H. Park, “Isobar of an ideal Bose gas within the grand canonical ensemble,” *Phys. Rev. A* **84** 023636 (2011).
- [14] J.-H. Park, “How many is different? Answer from ideal Bose gas,” *J. Phys. Conf. Ser.* **490** 012018 (2014), [arXiv:1310.5580 [cond-mat.stat-mech]], *c.f.* [16].

- [15] W. Cho, S. W. Kim and J.-H. Park, “Two-dimensional Bose-Einstein condensate under pressure,” *New J. Phys.* **17** (2015) no.1, 013038 doi:10.1088/1367-2630/17/1/013038 [arXiv:1409.4277 [cond-mat.quant-gas]].
- [16] P. W. Anderson, “More Is Different,” *Science* **177**, 393 (1972).
- [17] J. M. H. Levelt Sengers, “From Van der Waals’ equation to the scaling laws” *Physica* **73** 73 (1974). doi:10.1016/0031-8914(74)90227-4
- [18] G. Schmidt and H. Wenzel, “A modified van der Waals type equation of state,” *Chemical Engineering Science* **35** (1980) 1503 doi:10.1016/0009-2509(80)80044-3.

Supplementary Material for “Janus van der Waals equations for real molecules with two-sided phase transitions”

Jihwan Kim, Do-Hyun Kim, and Jeong-Hyuck Park

SM 1 SUPPLEMENTARY FIGURES FOR $N = 4$ CASE

SM 1.1 argon (Ar)

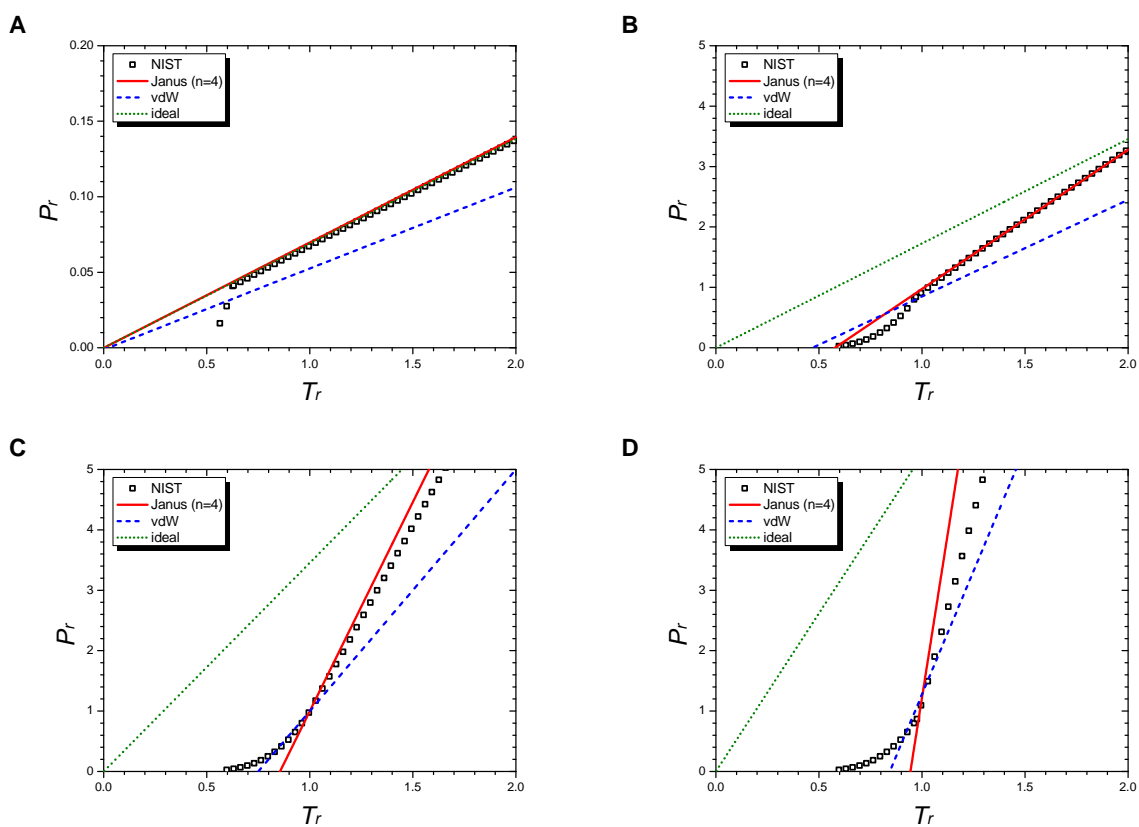


Figure S1. Isochoric curves of argon (Ar) at $1/v_r = 0.02$ (A), $1/v_r = 0.5$ (B), $1/v_r = 1.0$ (C), and $1/v_r = 1.5$ (D). Boxes are from the NIST data. The red solid line is drawn from the $n = 4$ Janus van der Waals equation, the blue dashed line from the original van der Waals equation, and the green dotted line from the classical ideal gas law.

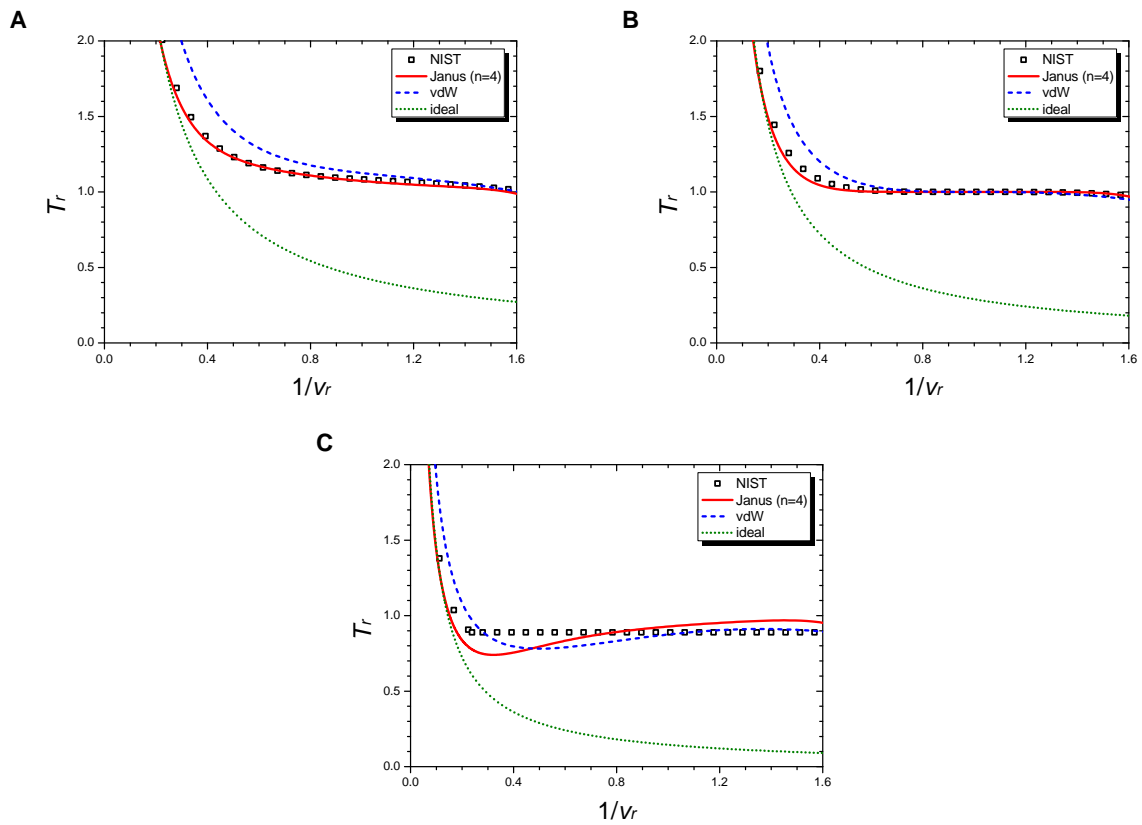


Figure S2. Isobaric curves of argon (Ar) at $P_r = 1.5$ (A), $P_r = 1.0$ (B), and $P_r = 0.5$ (C). Boxes are from the NIST data. The red solid line is drawn from the $n = 4$ Janus van der Waals equation, the blue dashed line from the original van der Waals equation, and the green dotted line from the classical ideal gas law.

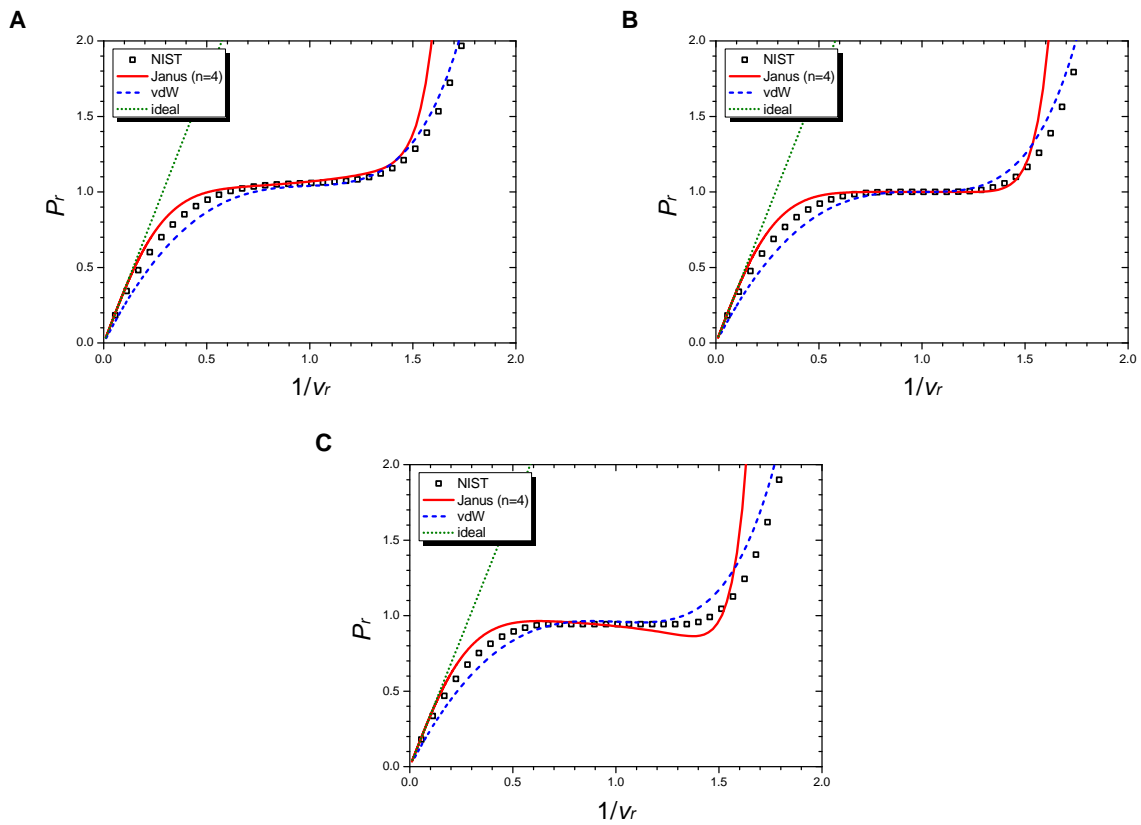


Figure S3. Isothermal curves of argon (Ar) at $T_r = 1.01$ (A), $T_r = 1.00$ (B), and $T_r = 0.99$ (C). Boxes are from the NIST data. The red solid line is drawn from the $n = 4$ Janus van der Waals equation, the blue dashed line from the original van der Waals equation, and the green dotted line from the classical ideal gas law.

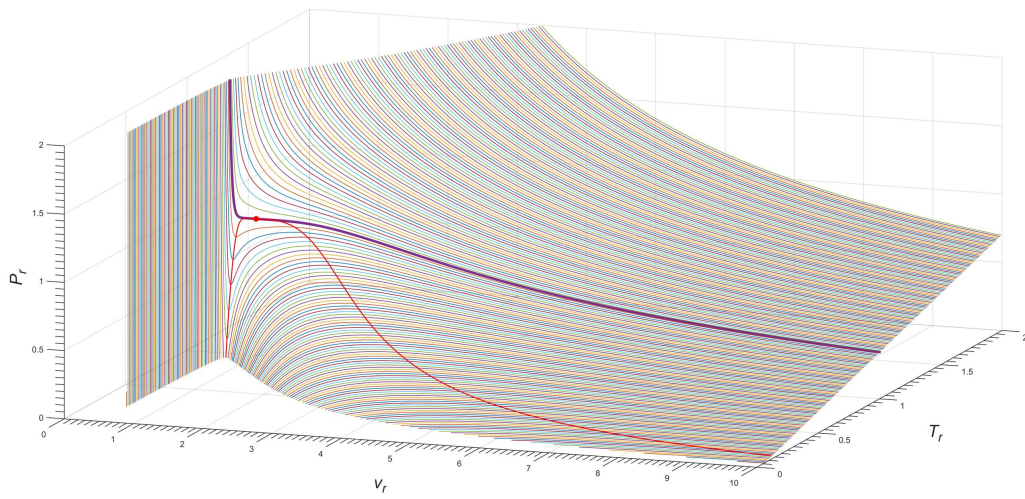


Figure S4. Three-dimensional $P_r - v_r - T_r$ phase diagram of the exact $n = 4$ Janus van der Waals equation, as for argon (Ar). The bold purple line corresponds to the isotherm of $T_r = 1.00$ as depicted in **Figure S3 B**; the red line is the Janus van der Waals spinodal curve with $a = 0.99$; and the red dot is the critical point.

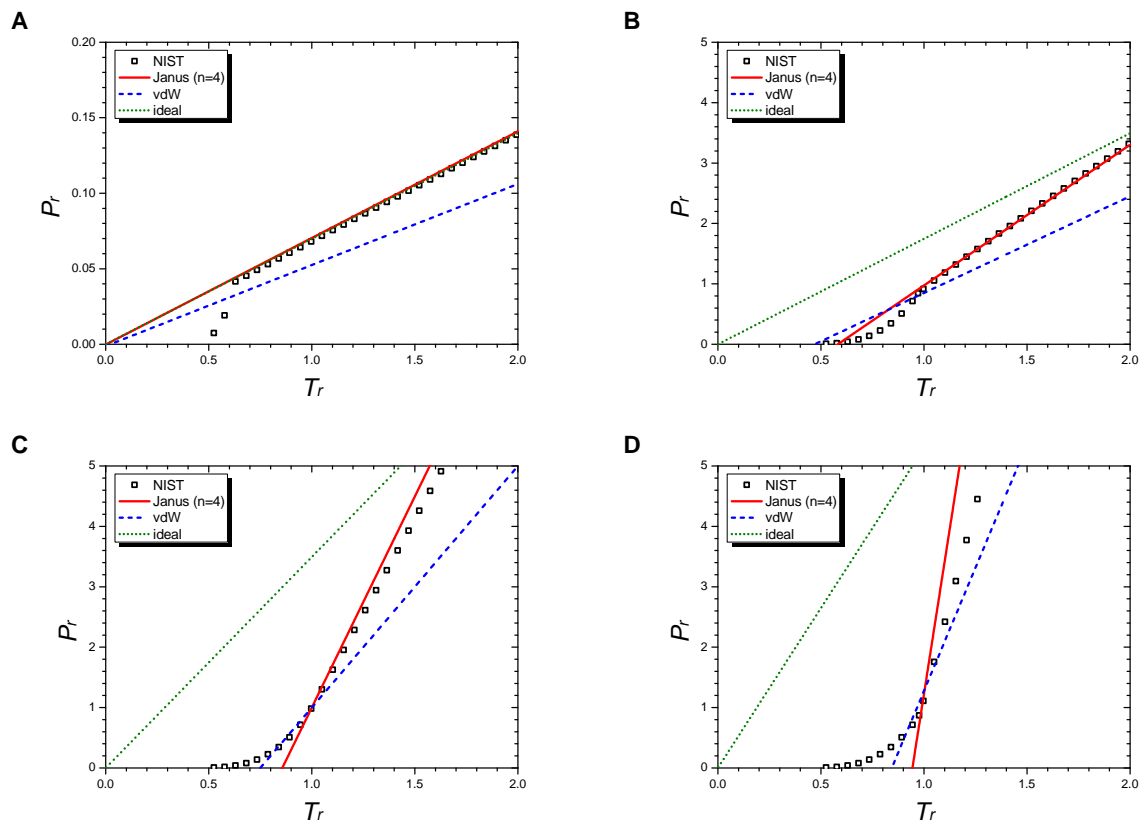
SM 1.2 methane (CH_4)

Figure S5. Isochoric curves of methane (CH_4) at $1/v_r = 0.02$ (**A**), $1/v_r = 0.5$ (**B**), $1/v_r = 1.0$ (**C**), and $1/v_r = 1.5$ (**D**). Boxes are from the NIST data. The red solid line is drawn from the $n = 4$ Janus van der Waals equation, the blue dashed line from the original van der Waals equation, and the green dotted line from the classical ideal gas law.

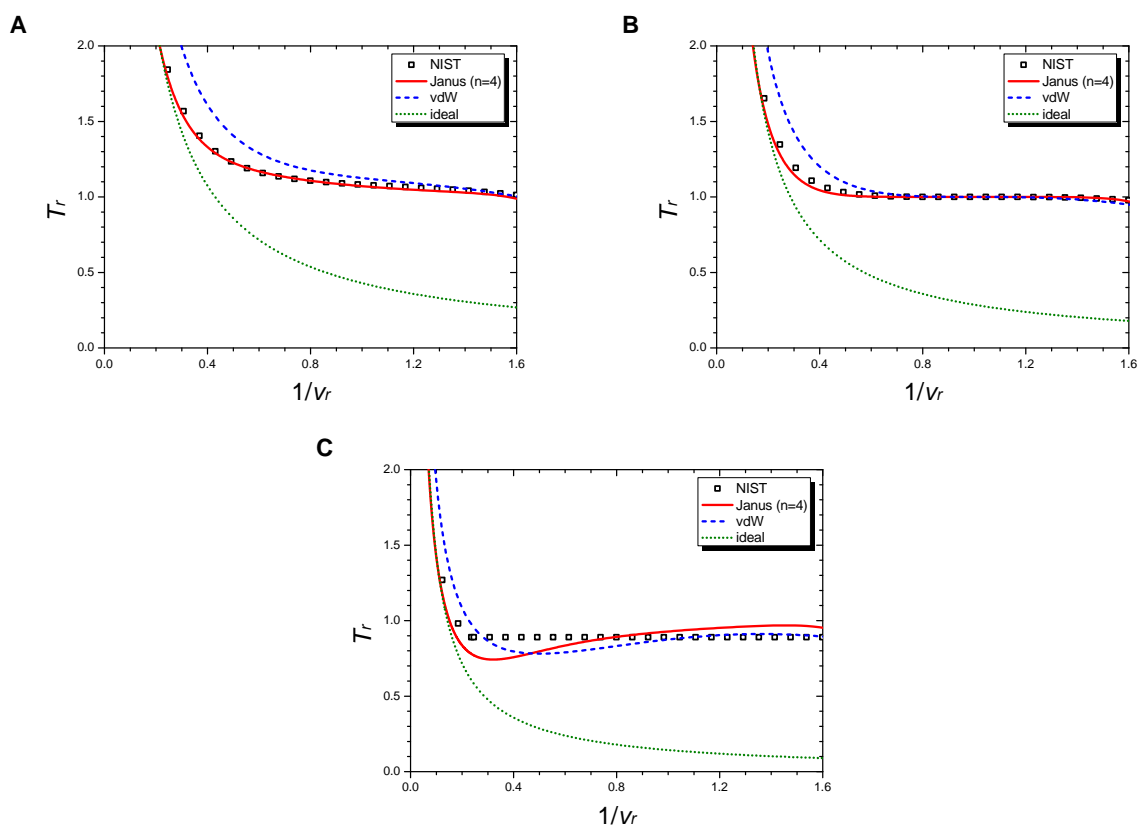


Figure S6. Isobaric curves of methane (CH₄) at $P_r = 1.5$ (A), $P_r = 1.0$ (B), and $P_r = 0.5$ (C). Boxes are from the NIST data. The red solid line is drawn from the $n = 4$ Janus van der Waals equation, the blue dashed line from the original van der Waals equation, and the green dotted line from the classical ideal gas law.

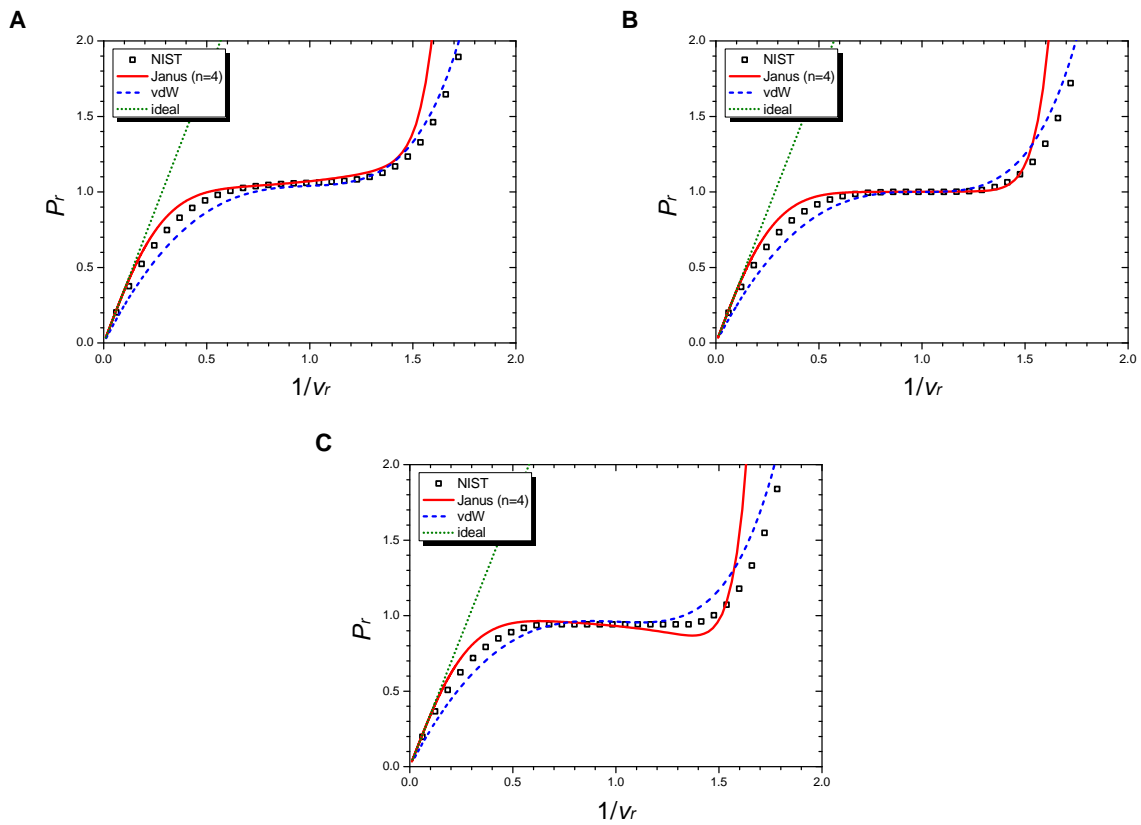


Figure S7. Isothermal curves of methane (CH_4) at $T_r = 1.01$ (A), $T_r = 1.00$ (B), and $T_r = 0.99$ (C). Boxes are from the NIST data. The red solid line is drawn from the $n = 4$ Janus van der Waals equation, the blue dashed line from the original van der Waals equation, and the green dotted line from the classical ideal gas law.

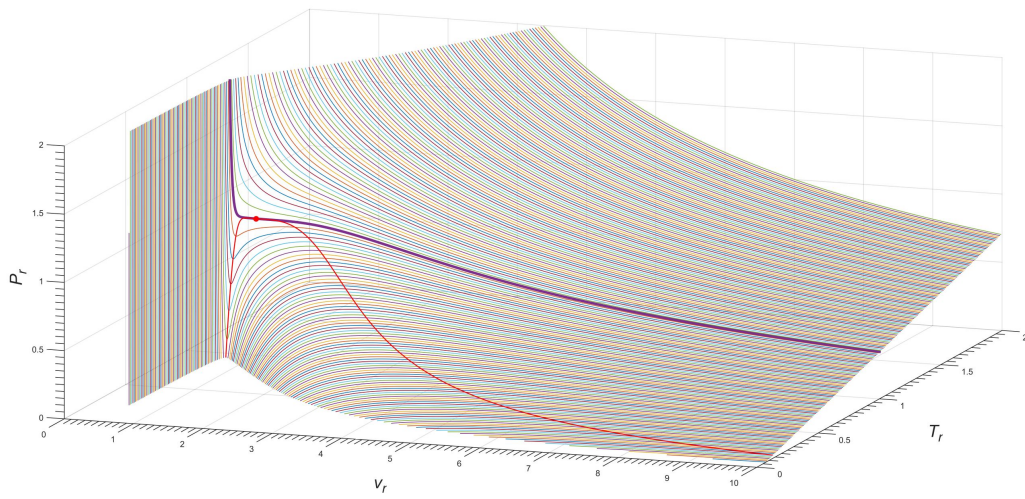


Figure S8. Three-dimensional $P_r - v_r - T_r$ phase diagram of the exact $n = 4$ Janus van der Waals equation, as for methane (CH₄). The bold purple line corresponds to the isotherm of $T_r = 1.00$ as depicted in **Figure S7 B**; the red line is the Janus van der Waals spinodal curve with $a = 0.99$; and the red dot is the critical point.

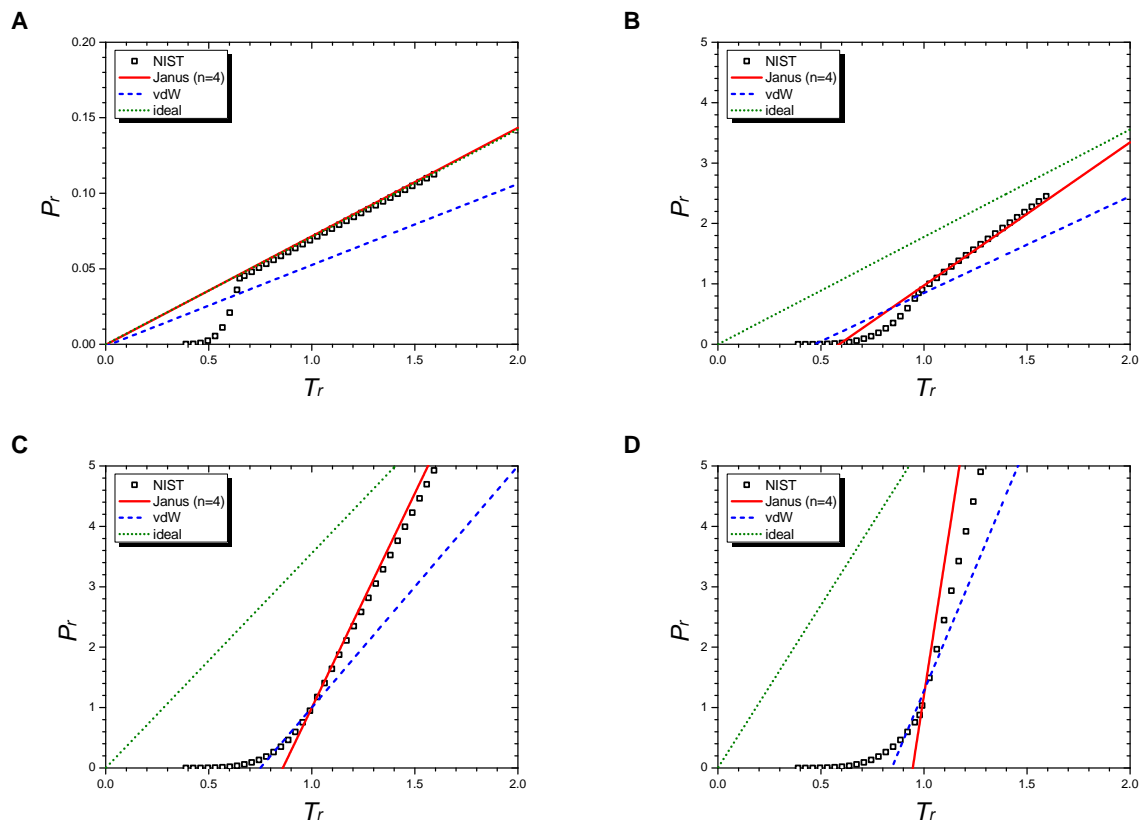
SM 1.3 ethylene (C_2H_4)

Figure S9. Isochoric curves of ethylene (C_2H_4) at $1/v_r = 0.02$ (**A**), $1/v_r = 0.5$ (**B**), $1/v_r = 1.0$ (**C**), and $1/v_r = 1.5$ (**D**). Boxes are from the NIST data. The red solid line is drawn from the $n = 4$ Janus van der Waals equation, the blue dashed line from the original van der Waals equation, and the green dotted line from the classical ideal gas law.

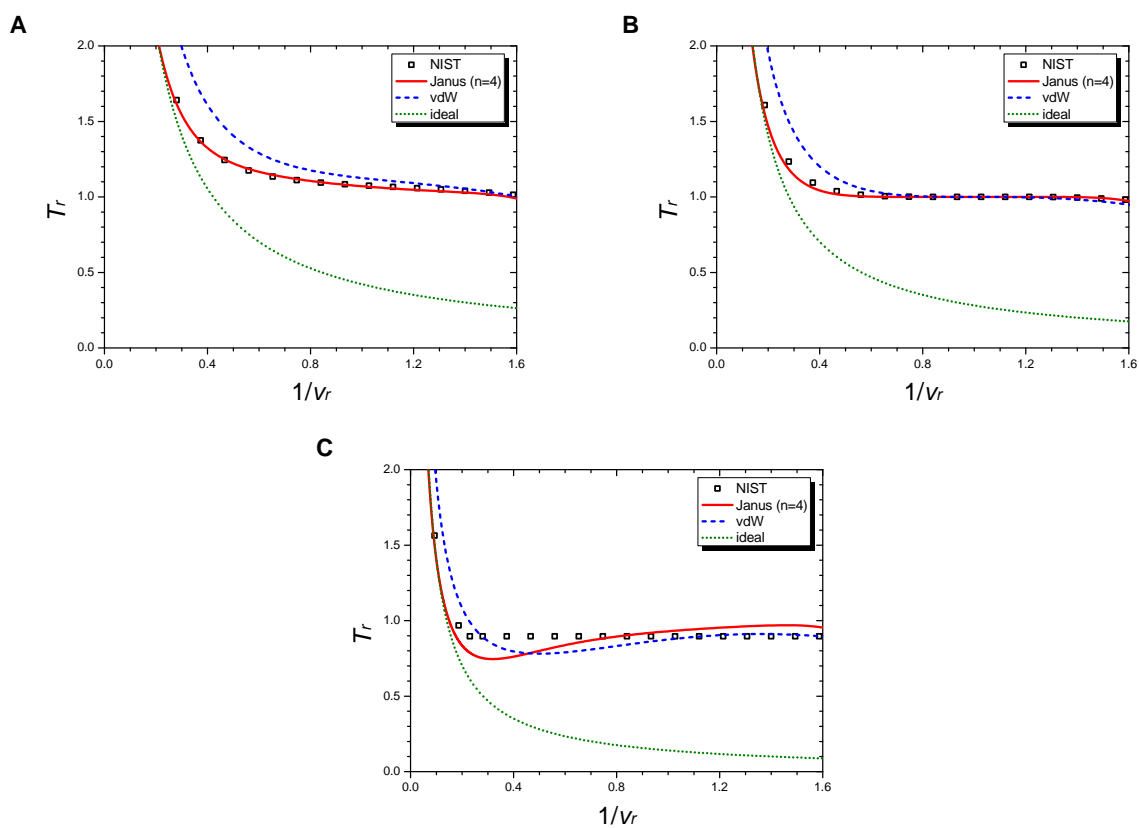


Figure S10. Isobaric curves of ethylene (C_2H_4) at $P_r = 1.5$ (A), $P_r = 1.0$ (B), and $P_r = 0.5$ (C). Boxes are from the NIST data. The red solid line is drawn from the $n = 4$ Janus van der Waals equation, the blue dashed line from the original van der Waals equation, and the green dotted line from the classical ideal gas law.

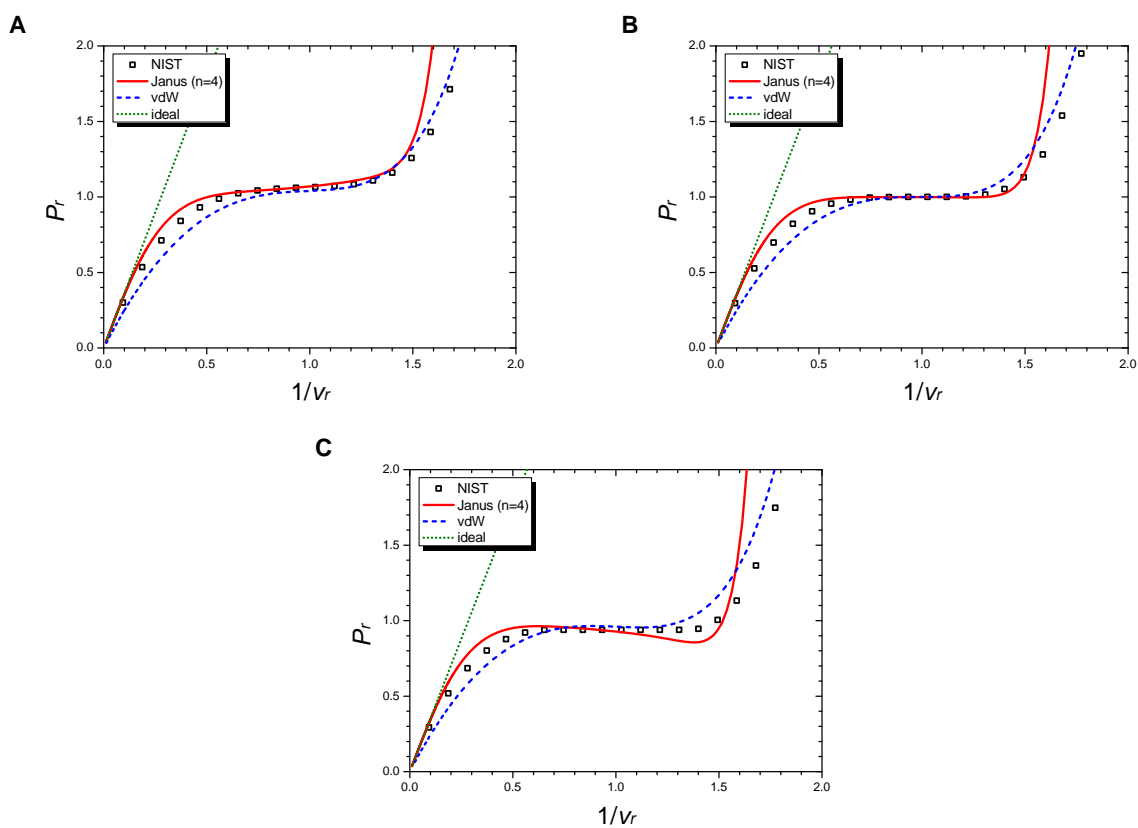


Figure S11. Isothermal curves of ethylene (C_2H_4) at $T_r = 1.01$ (A), $T_r = 1.00$ (B), and $T_r = 0.99$ (C). Boxes are from the NIST data. The red solid line is drawn from the $n = 4$ Janus van der Waals equation, the blue dashed line from the original van der Waals equation, and the green dotted line from the classical ideal gas law.

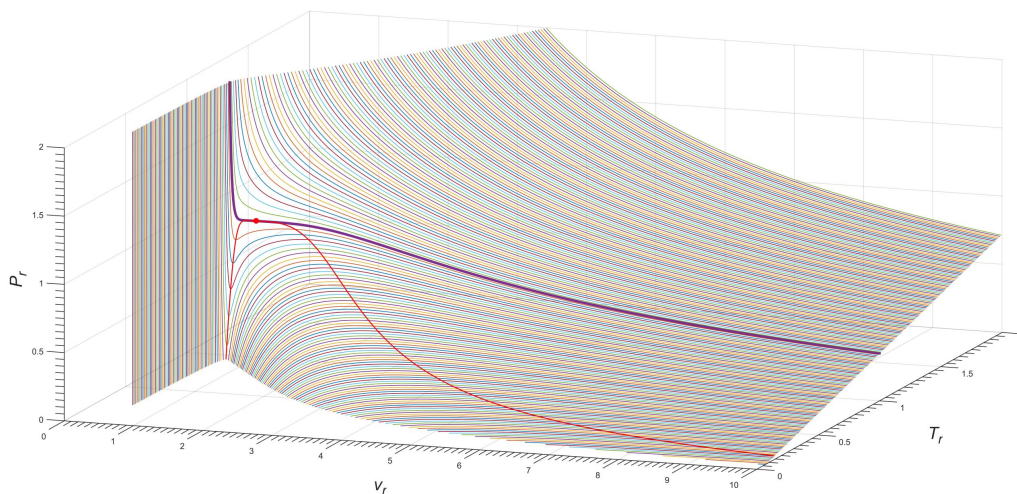


Figure S12. Three-dimensional $P_r - v_r - T_r$ phase diagram of the exact $n = 4$ Janus van der Waals equation, as for ethylene (C_2H_4). The bold purple line corresponds to the isotherm of $T_r = 1.00$ as depicted in **Figure S11 B**; the red line is the Janus van der Waals spinodal curve with $a = 0.99$; and the red dot is the critical point.

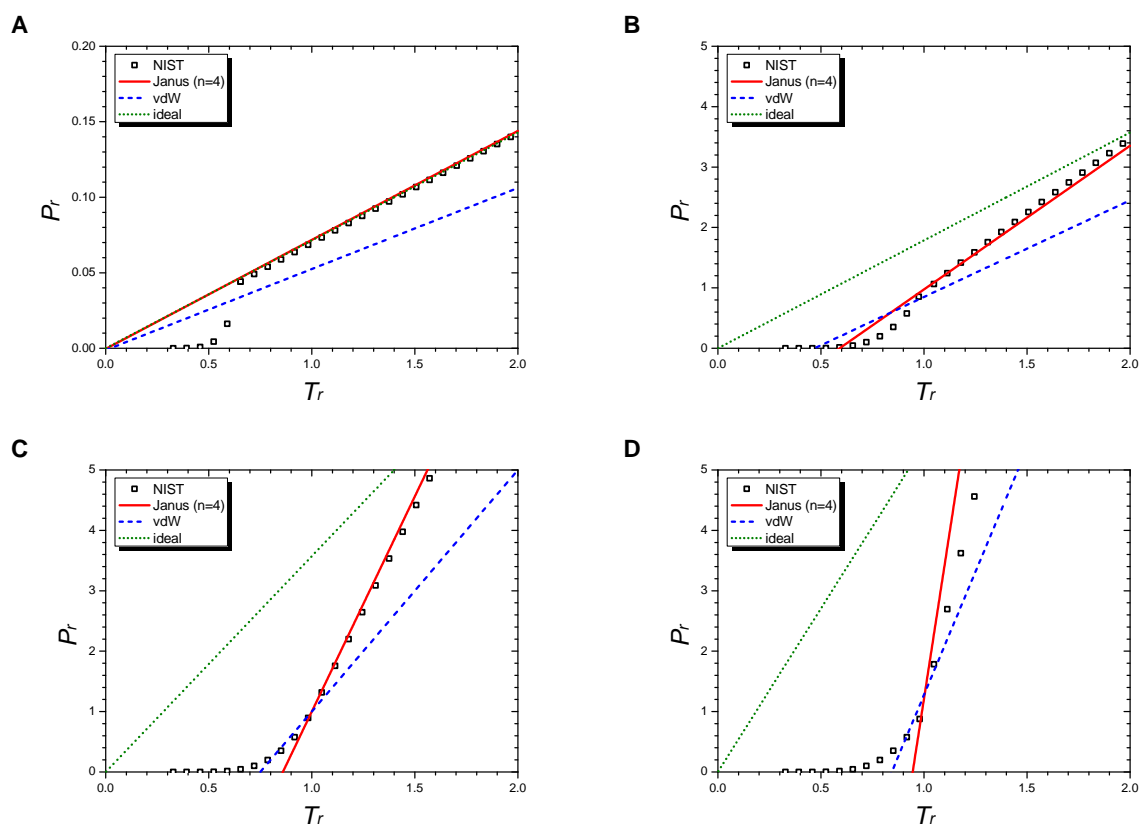
SM 1.4 ethane (C_2H_6)

Figure S13. Isochoric curves of ethane (C_2H_6) at $1/v_r = 0.02$ (A), $1/v_r = 0.5$ (B), $1/v_r = 1.0$ (C), and $1/v_r = 1.5$ (D). Boxes are from the NIST data. The red solid line is drawn from the $n = 4$ Janus van der Waals equation, the blue dashed line from the original van der Waals equation, and the green dotted line from the classical ideal gas law.

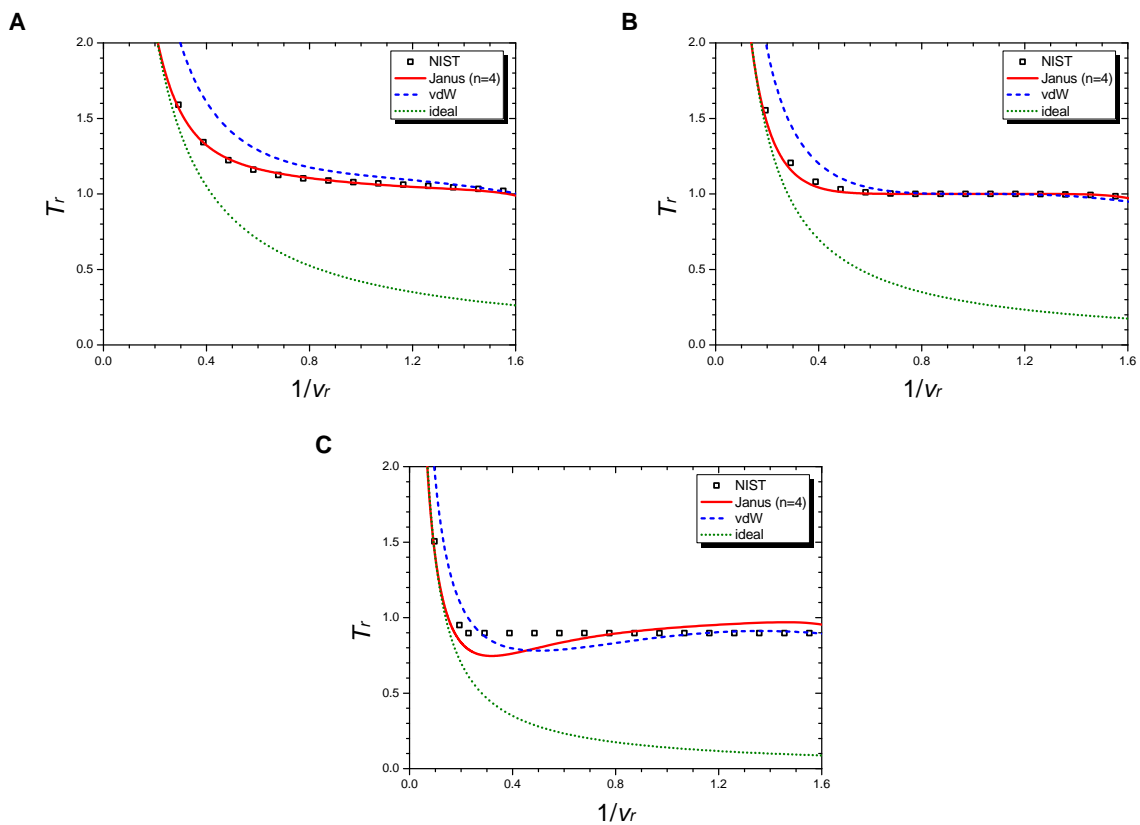


Figure S14. Isobaric curves of ethane (C_2H_6) at $P_r = 1.5$ (A), $P_r = 1.0$ (B), and $P_r = 0.5$ (C). Boxes are from the NIST data. The red solid line is drawn from the $n = 4$ Janus van der Waals equation, the blue dashed line from the original van der Waals equation, and the green dotted line from the classical ideal gas law.

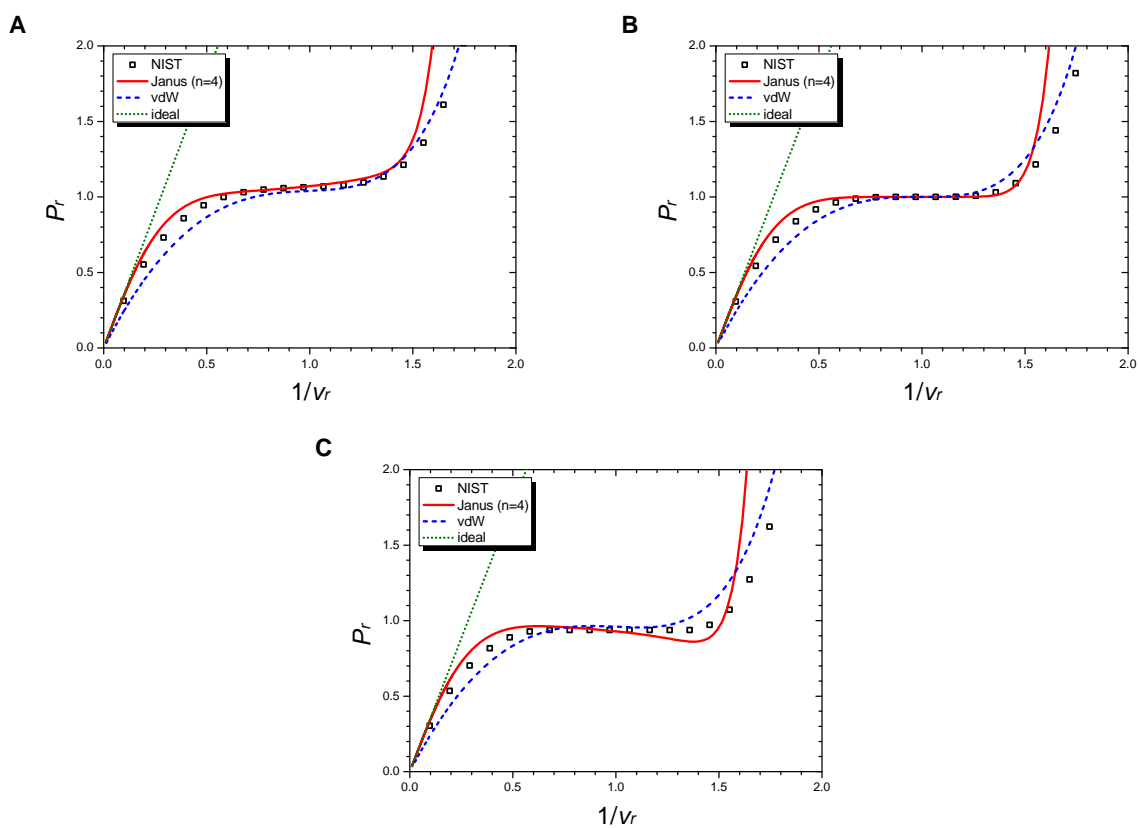


Figure S15. Isothermal curves of ethane (C_2H_6) at $T_r = 1.01$ (A), $T_r = 1.00$ (B), and $T_r = 0.99$ (C). Boxes are from the NIST data. The red solid line is drawn from the $n = 4$ Janus van der Waals equation, the blue dashed line from the original van der Waals equation, and the green dotted line from the classical ideal gas law.

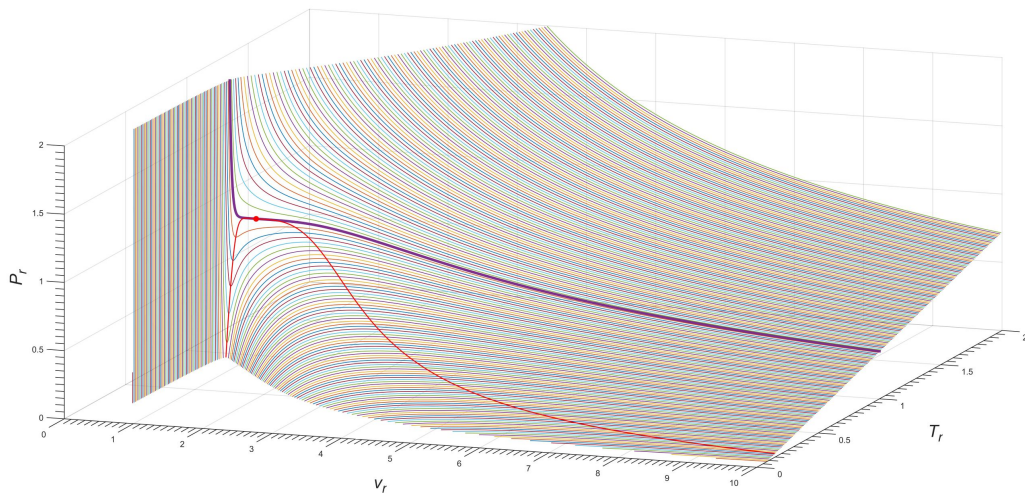


Figure S16. Three-dimensional $P_r - v_r - T_r$ phase diagram of the exact $n = 4$ Janus van der Waals equation, as for ethane (C_2H_6). The bold purple line corresponds to the isotherm of $T_r = 1.00$ as depicted in **Figure S15 B**; the red line is the Janus van der Waals spinodal curve with $a = 0.99$; and the red dot is the critical point.

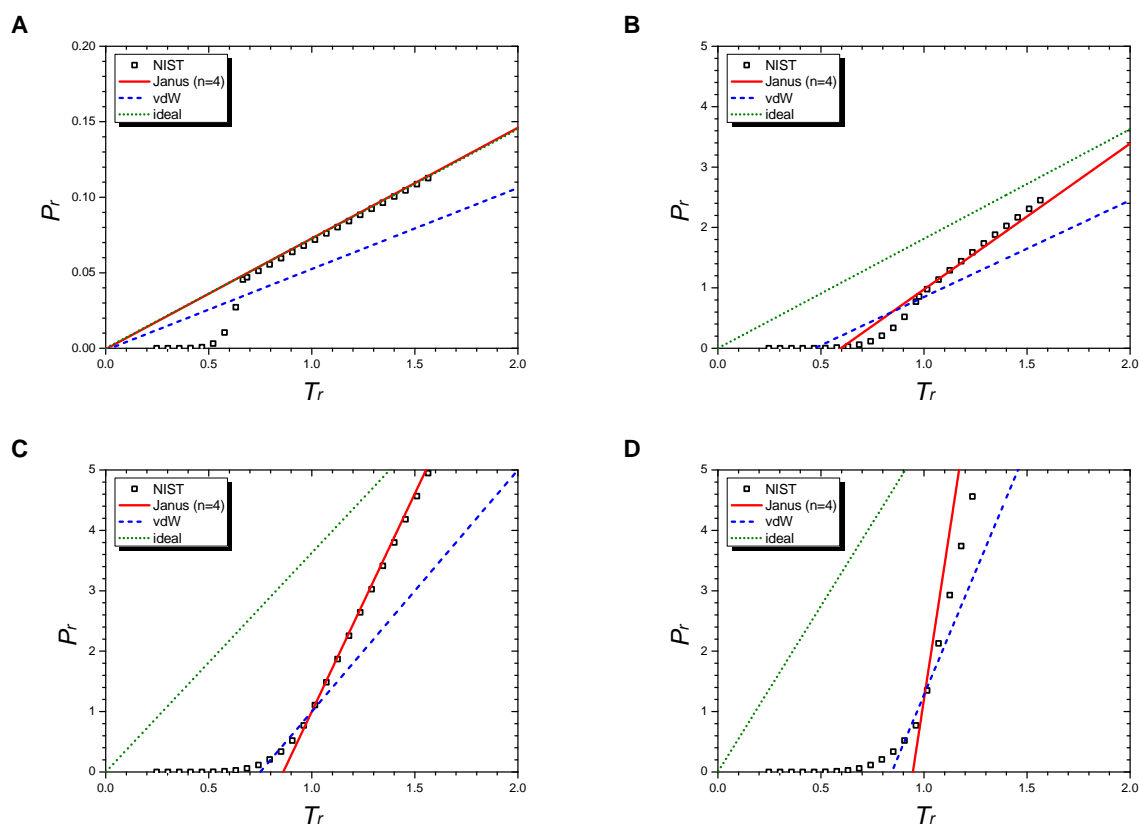
SM 1.5 propylene (C_3H_6)

Figure S17. Isochoric curves of propylene (C_3H_6) at $1/v_r = 0.02$ (A), $1/v_r = 0.5$ (B), $1/v_r = 1.0$ (C), and $1/v_r = 1.5$ (D). Boxes are from the NIST data. The red solid line is drawn from the $n = 4$ Janus van der Waals equation, the blue dashed line from the original van der Waals equation, and the green dotted line from the classical ideal gas law.

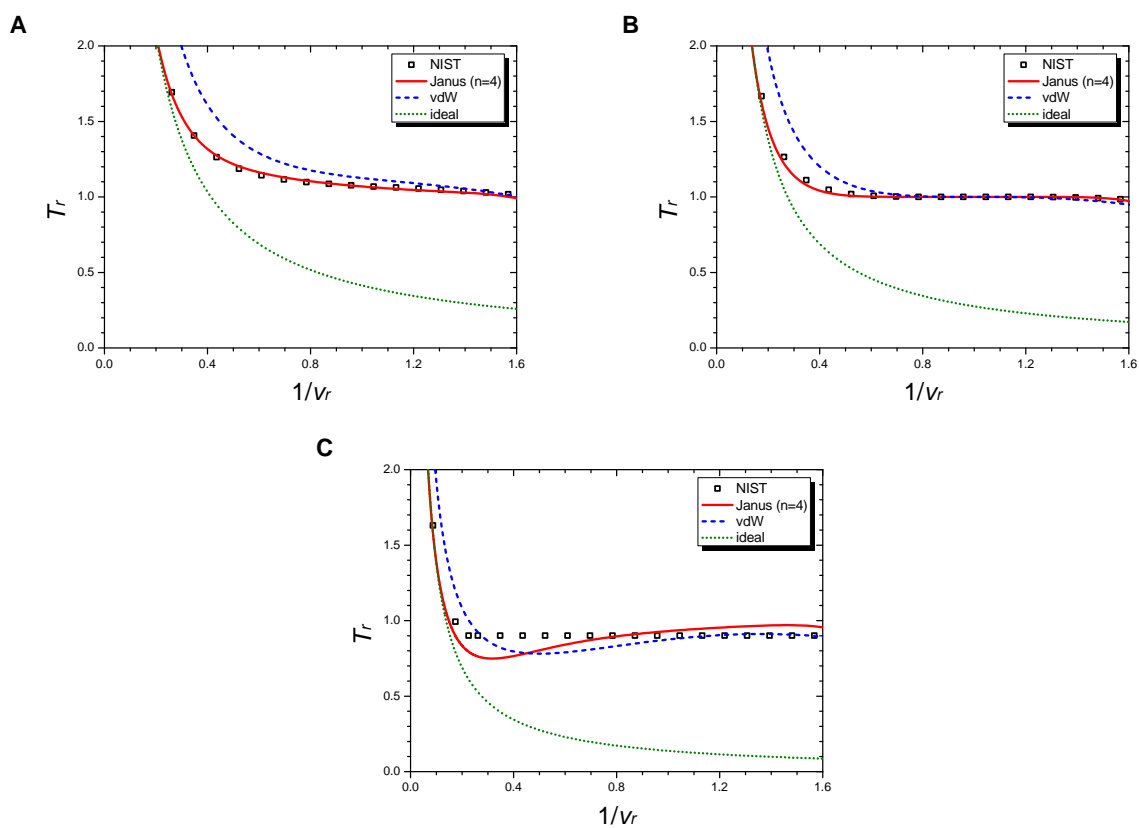


Figure S18. Isobaric curves of propylene (C_3H_6) at $P_r = 1.5$ (A), $P_r = 1.0$ (B), and $P_r = 0.5$ (C). Boxes are from the NIST data. The red solid line is drawn from the $n = 4$ Janus van der Waals equation, the blue dashed line from the original van der Waals equation, and the green dotted line from the classical ideal gas law.

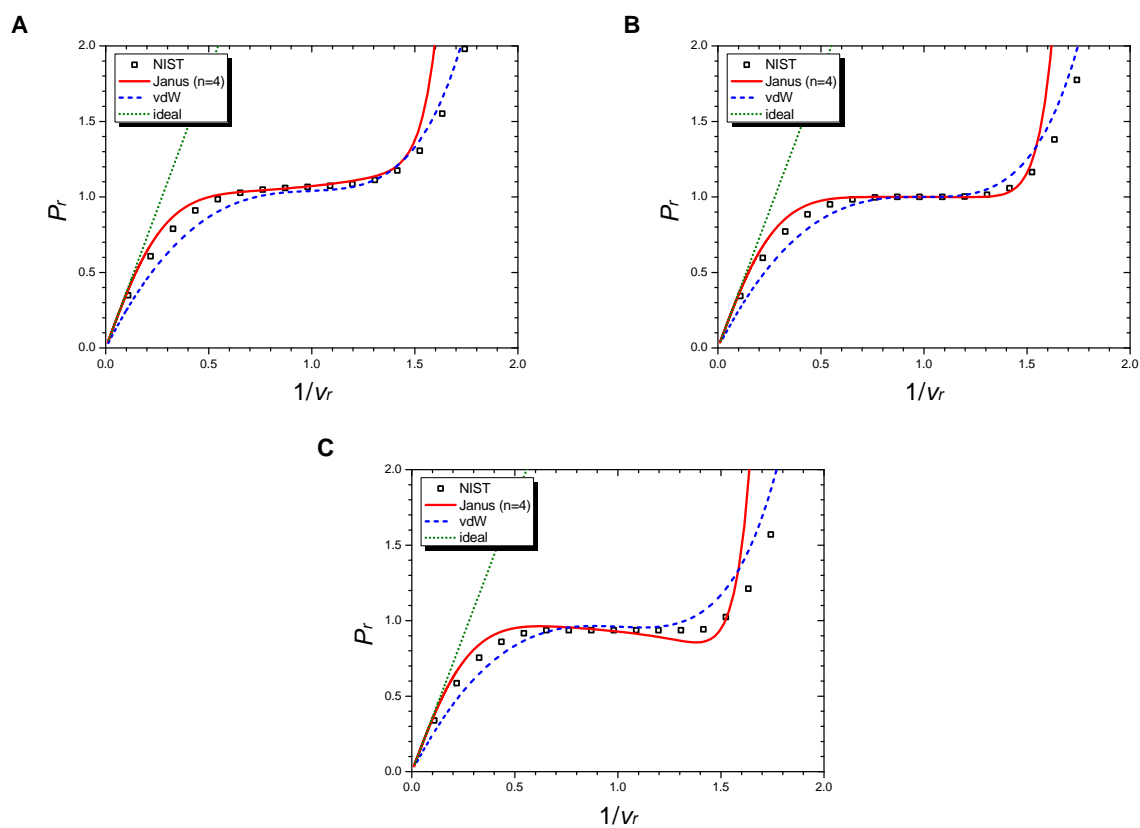


Figure S19. Isothermal curves of propylene (C_3H_6) at $T_r = 1.01$ (A), $T_r = 1.00$ (B), and $T_r = 0.99$ (C). Boxes are from the NIST data. The red solid line is drawn from the $n = 4$ Janus van der Waals equation, the blue dashed line from the original van der Waals equation, and the green dotted line from the classical ideal gas law.

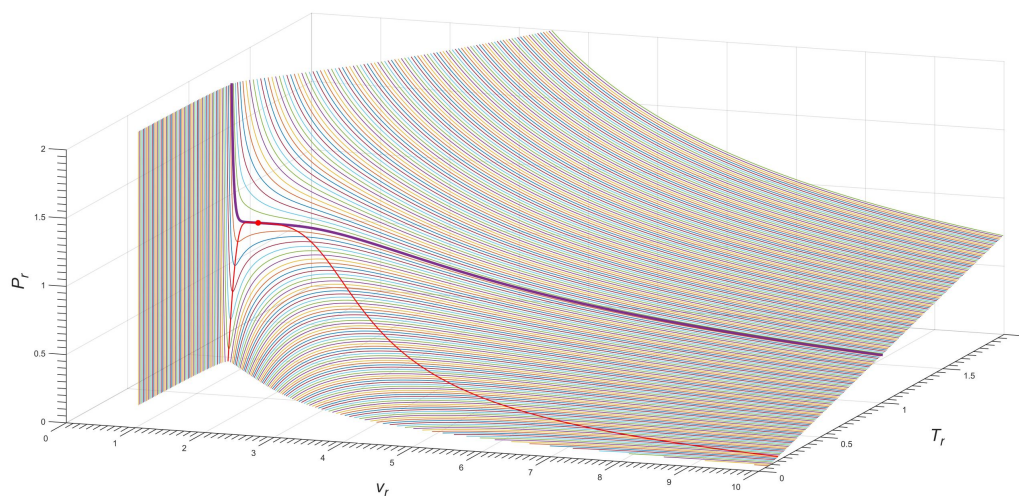


Figure S20. Three-dimensional $P_r - v_r - T_r$ phase diagram of the exact $n = 4$ Janus van der Waals equation, as for propylene (C_3H_6). The bold purple line corresponds to the isotherm of $T_r = 1.00$ as depicted in **Figure S19 B**; the red line is the Janus van der Waals spinodal curve with $a = 0.99$; and the red dot is the critical point.

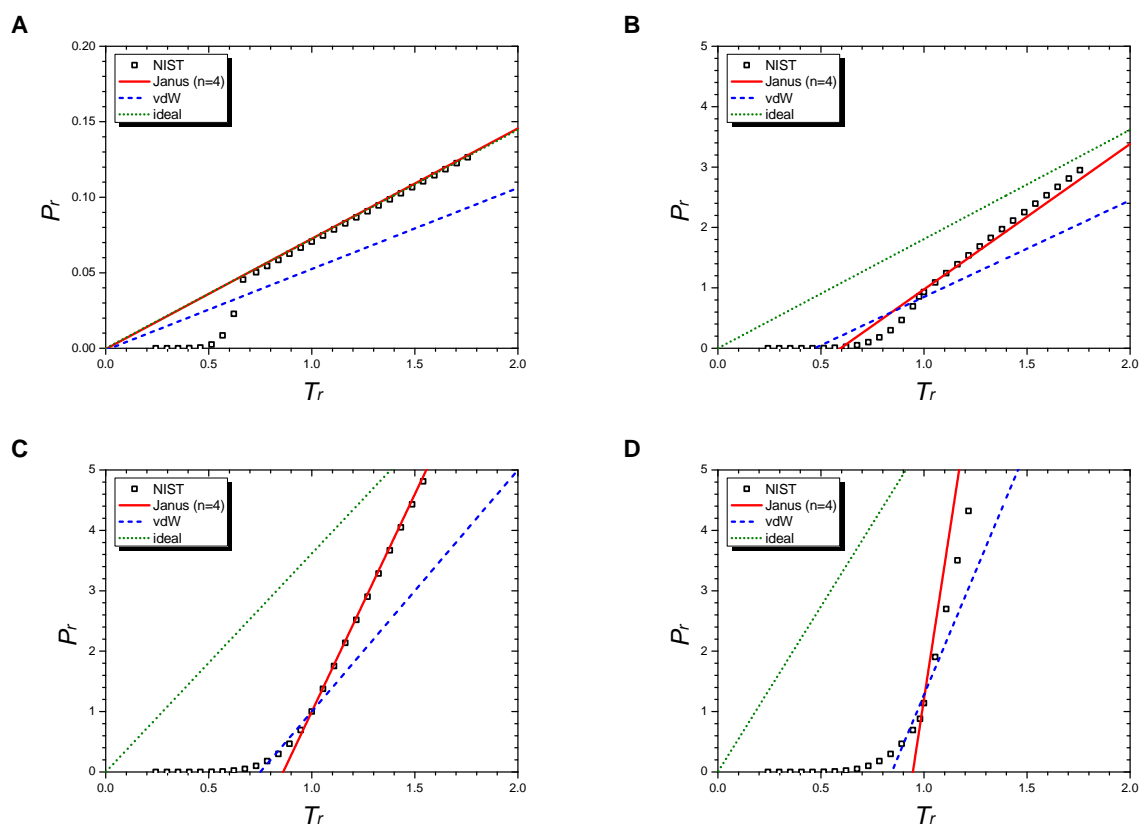
SM 1.6 propane (C_3H_8)

Figure S21. Isochoric curves of propane (C_3H_8) at $1/v_r = 0.02$ (A), $1/v_r = 0.5$ (B), $1/v_r = 1.0$ (C), and $1/v_r = 1.5$ (D). Boxes are from the NIST data. The red solid line is drawn from the $n = 4$ Janus van der Waals equation, the blue dashed line from the original van der Waals equation, and the green dotted line from the classical ideal gas law.

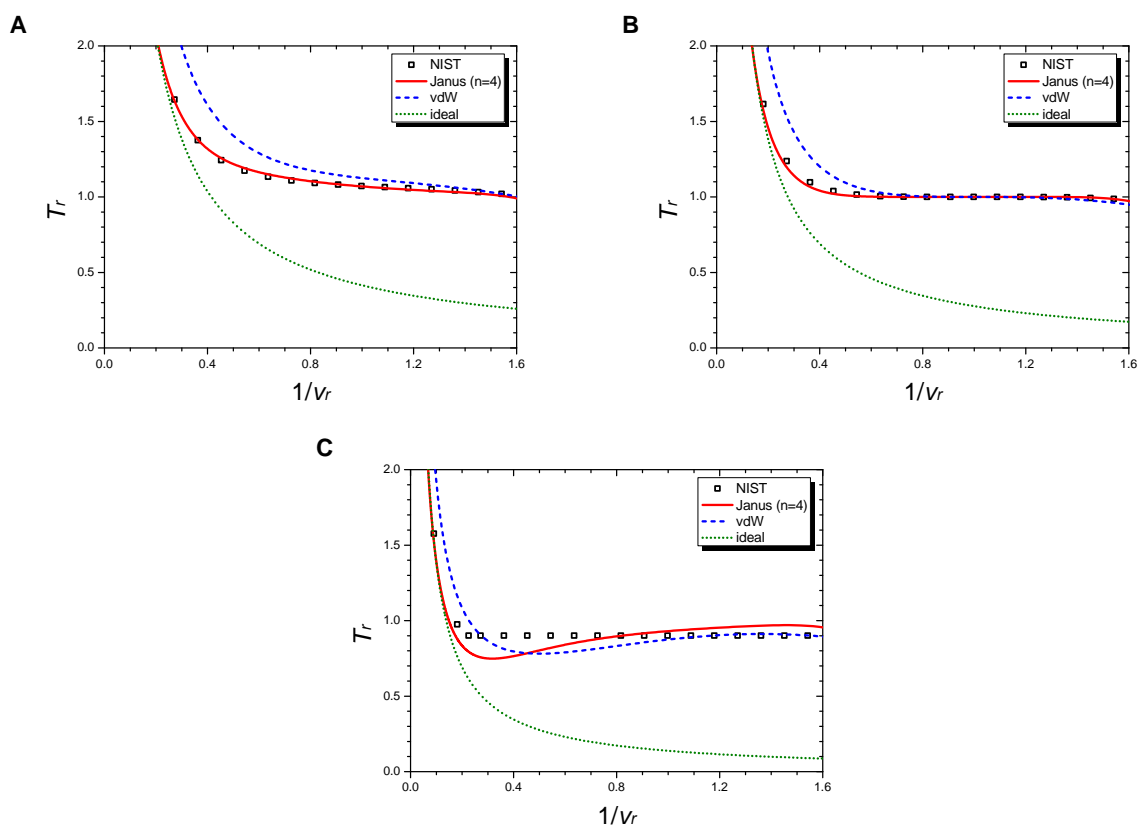


Figure S22. Isobaric curves of propane (C_3H_8) at $P_r = 1.5$ (A), $P_r = 1.0$ (B), and $P_r = 0.5$ (C). Boxes are from the NIST data. The red solid line is drawn from the $n = 4$ Janus van der Waals equation, the blue dashed line from the original van der Waals equation, and the green dotted line from the classical ideal gas law.

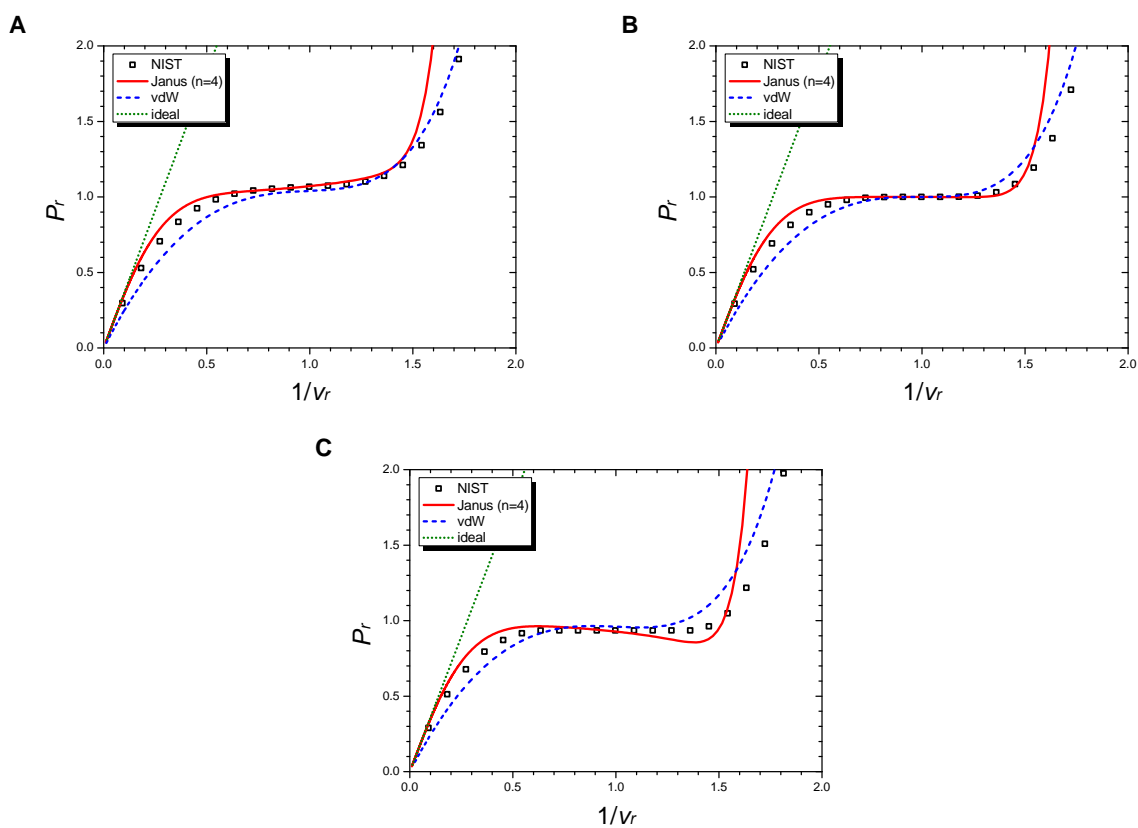


Figure S23. Isothermal curves of propane (C_3H_8) at $T_r = 1.01$ (A), $T_r = 1.00$ (B), and $T_r = 0.99$ (C). Boxes are from the NIST data. The red solid line is drawn from the $n = 4$ Janus van der Waals equation, the blue dashed line from the original van der Waals equation, and the green dotted line from the classical ideal gas law.

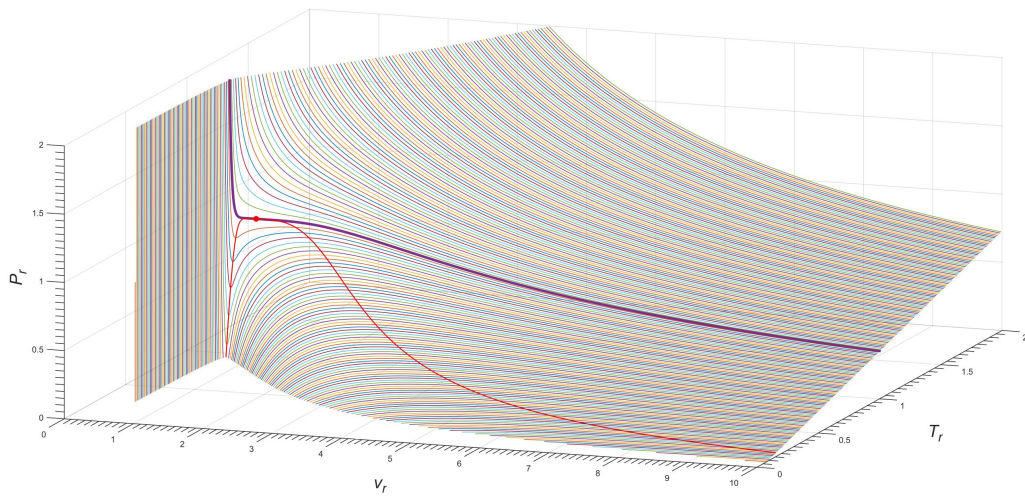


Figure S24. Three-dimensional $P_r - v_r - T_r$ phase diagram of the exact $n = 4$ Janus van der Waals equation, as for propane (C_3H_8). The bold purple line corresponds to the isotherm of $T_r = 1.00$ as depicted in **Figure S23 B**; the red line is the Janus van der Waals spinodal curve with $a = 0.99$; and the red dot is the critical point.

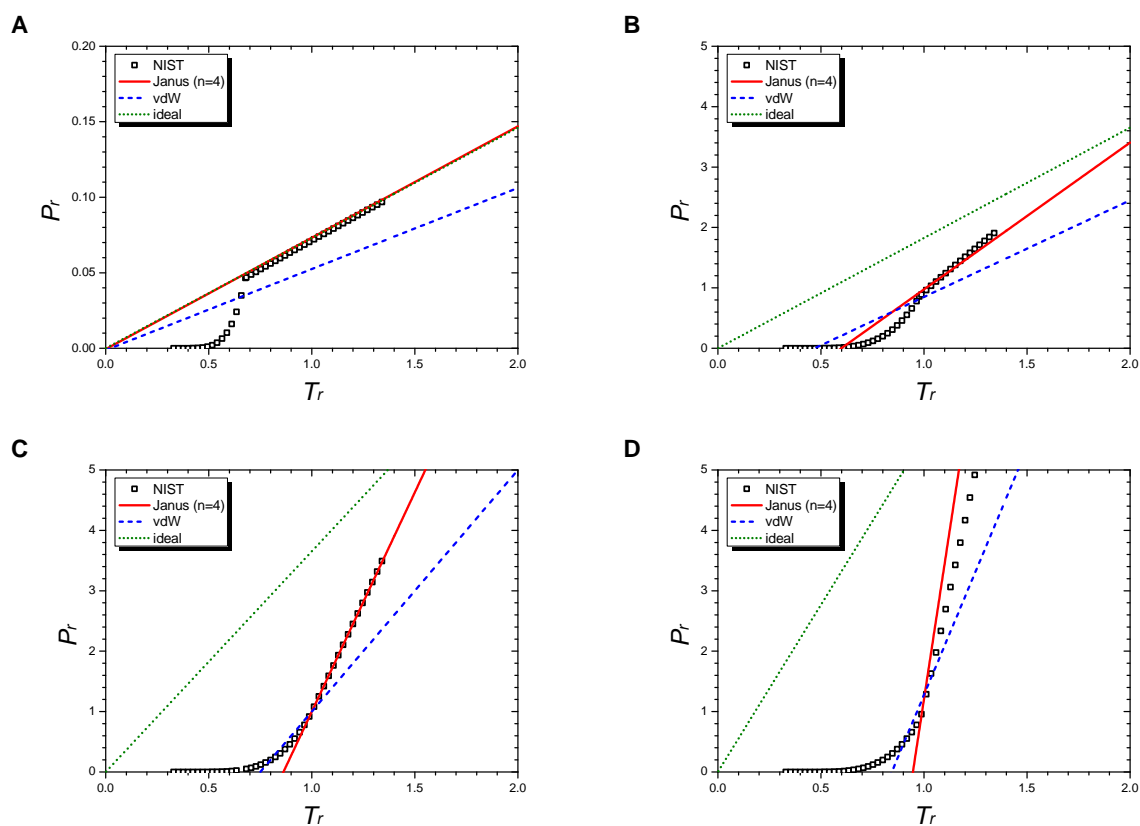
SM 1.7 butane (C_4H_{10})

Figure S25. Isochoric curves of butane (C_4H_{10}) at $1/v_r = 0.02$ (A), $1/v_r = 0.5$ (B), $1/v_r = 1.0$ (C), and $1/v_r = 1.5$ (D). Boxes are from the NIST data. The red solid line is drawn from the $n = 4$ Janus van der Waals equation, the blue dashed line from the original van der Waals equation, and the green dotted line from the classical ideal gas law.

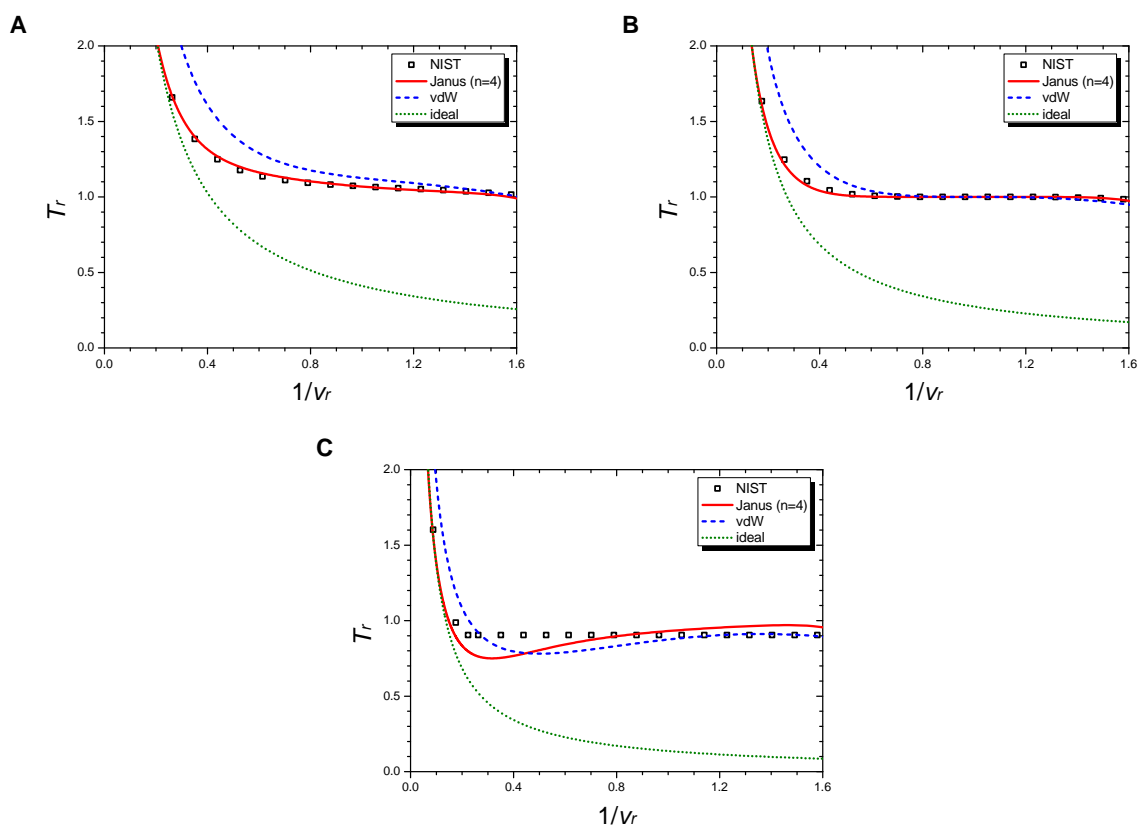


Figure S26. Isobaric curves of butane (C_4H_{10}) at $P_r = 1.5$ (A), $P_r = 1.0$ (B), and $P_r = 0.5$ (C). Boxes are from the NIST data. The red solid line is drawn from the $n = 4$ Janus van der Waals equation, the blue dashed line from the original van der Waals equation, and the green dotted line from the classical ideal gas law.

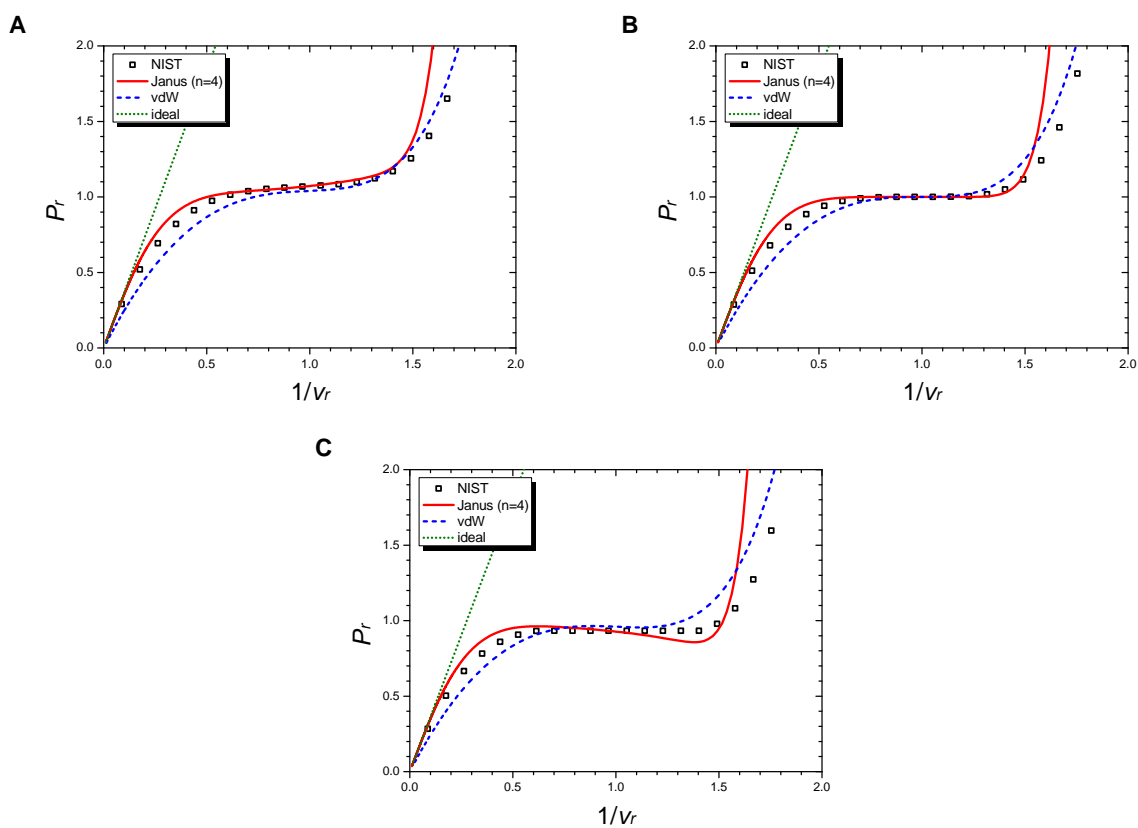


Figure S27. Isothermal curves of butane (C_4H_{10}) at $T_r = 1.01$ (A), $T_r = 1.00$ (B), and $T_r = 0.99$ (C). Boxes are from the NIST data. The red solid line is drawn from the $n = 4$ Janus van der Waals equation, the blue dashed line from the original van der Waals equation, and the green dotted line from the classical ideal gas law.

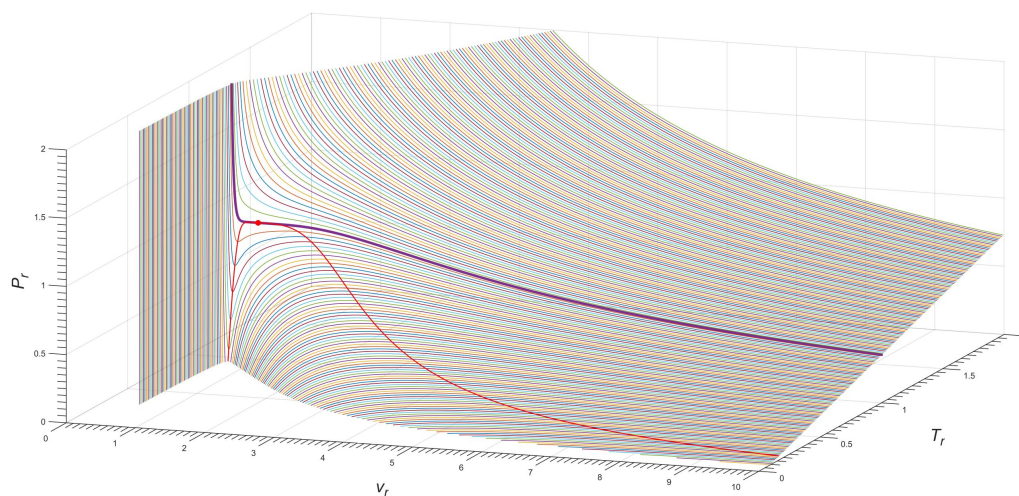


Figure S28. Three-dimensional $P_r - v_r - T_r$ phase diagram of the exact $n = 4$ Janus van der Waals equation, as for butane (C_4H_{10}). The bold purple line corresponds to the isotherm of $T_r = 1.00$ as depicted in **Figure S27 B**; the red line is the Janus van der Waals spinodal curve with $a = 0.99$; and the red dot is the critical point.

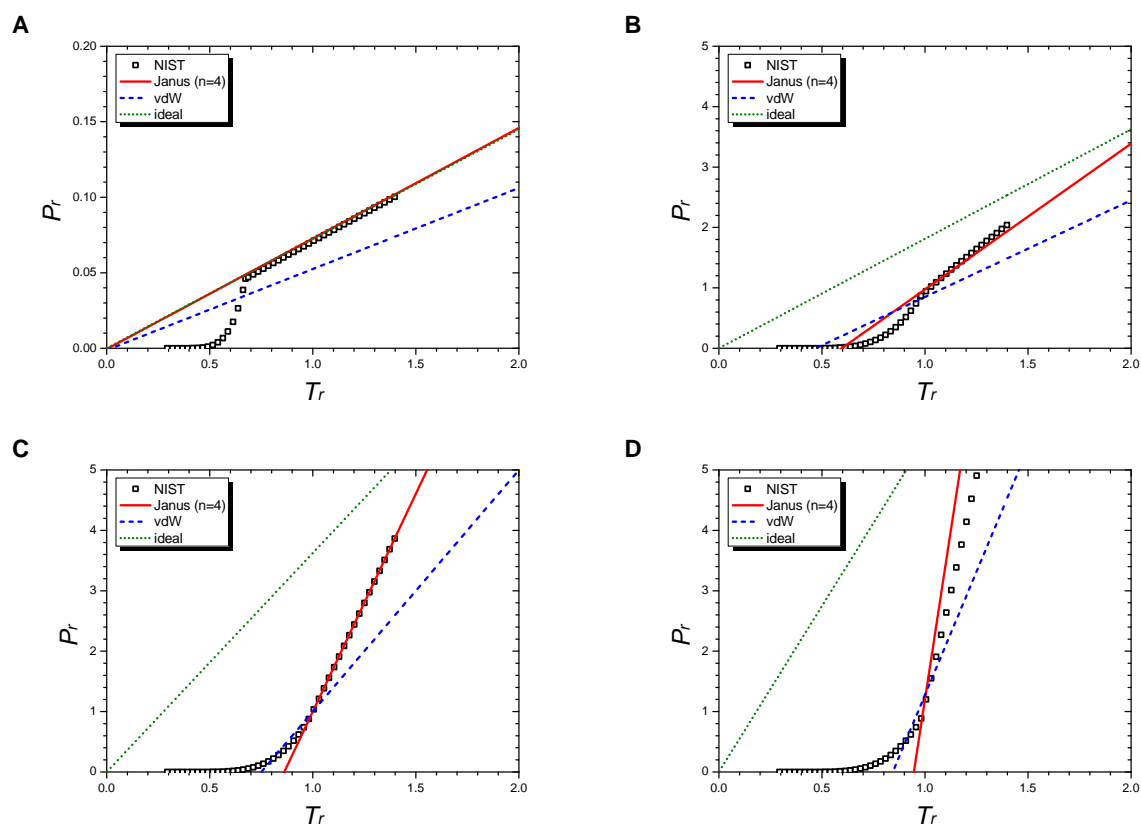
SM 1.8 isobutane (C_4H_{10})

Figure S29. Isochoric curves of isobutane (C_4H_{10}) at $1/v_r = 0.02$ (A), $1/v_r = 0.5$ (B), $1/v_r = 1.0$ (C), and $1/v_r = 1.5$ (D). Boxes are from the NIST data. The red solid line is drawn from the $n = 4$ Janus van der Waals equation, the blue dashed line from the original van der Waals equation, and the green dotted line from the classical ideal gas law.

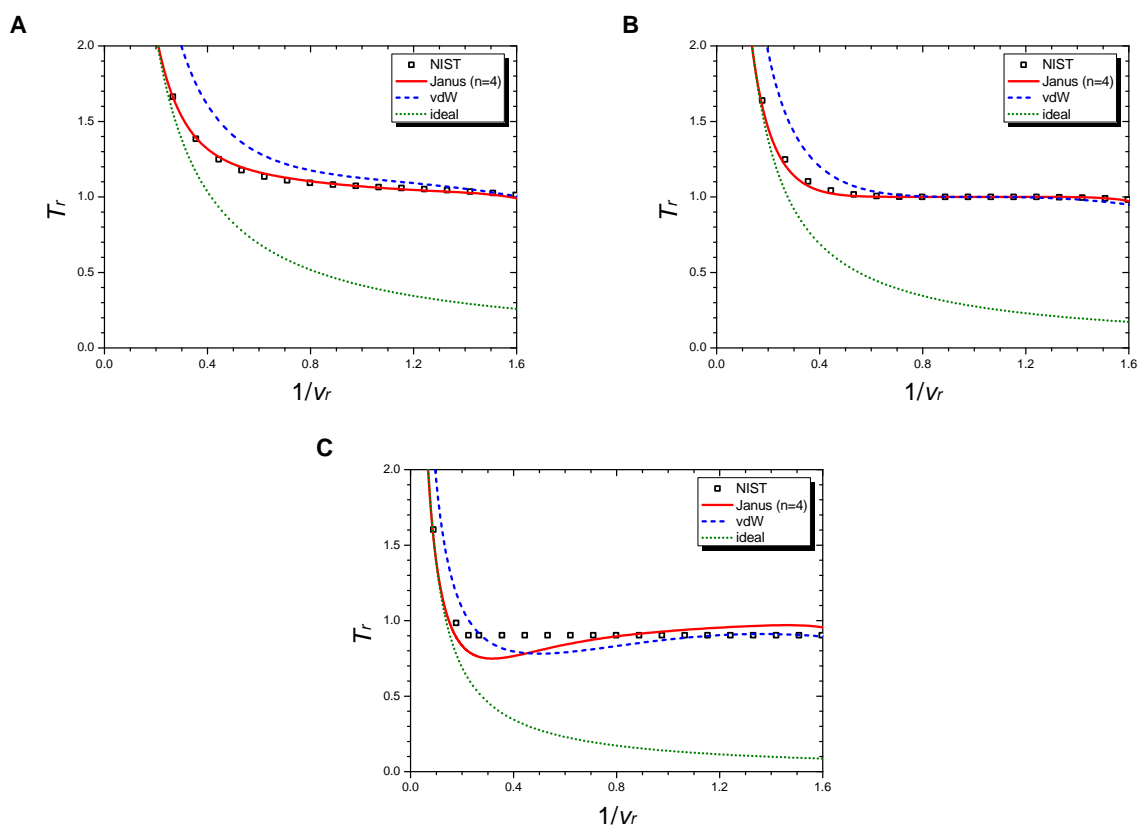


Figure S30. Isobaric curves of isobutane (C_4H_{10}) at $P_r = 1.5$ (A), $P_r = 1.0$ (B), and $P_r = 0.5$ (C). Boxes are from the NIST data. The red solid line is drawn from the $n = 4$ Janus van der Waals equation, the blue dashed line from the original van der Waals equation, and the green dotted line from the classical ideal gas law.

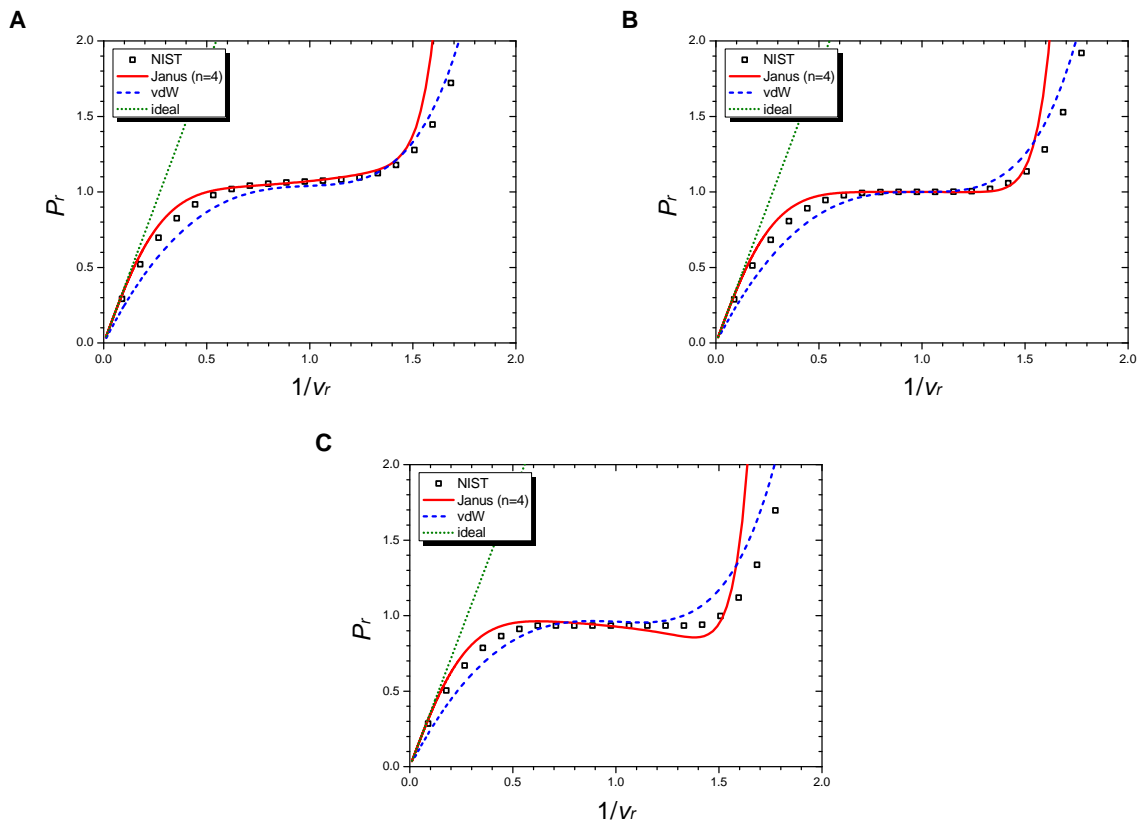


Figure S31. Isothermal curves of isobutane (C_4H_{10}) at $T_r = 1.01$ (A), $T_r = 1.00$ (B), and $T_r = 0.99$ (C). Boxes are from the NIST data. The red solid line is drawn from the $n = 4$ Janus van der Waals equation, the blue dashed line from the original van der Waals equation, and the green dotted line from the classical ideal gas law.

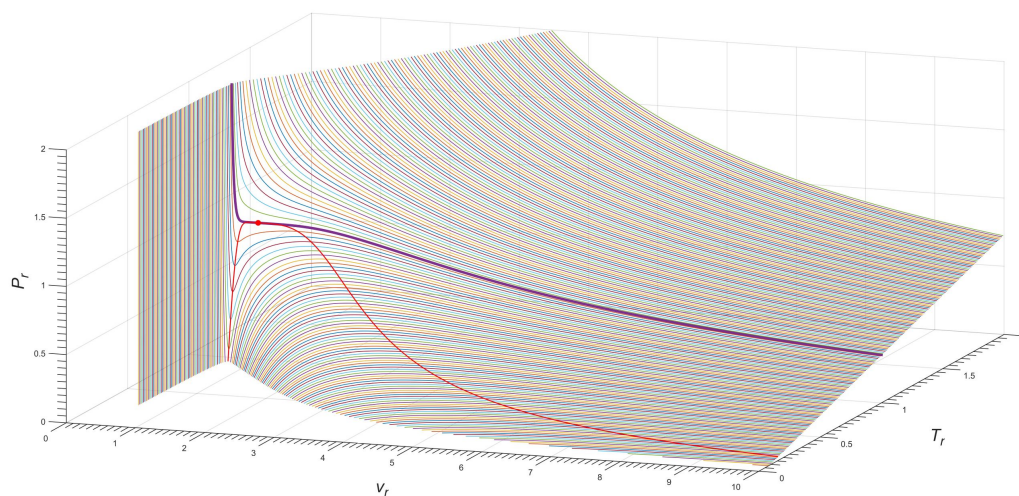


Figure S32. Three-dimensional $P_r - v_r - T_r$ phase diagram of the exact $n = 4$ Janus van der Waals equation, as for isobutane (C₄H₁₀). The bold purple line corresponds to the isotherm of $T_r = 1.00$ as depicted in **Figure S31 B**; the red line is the Janus van der Waals spinodal curve with $a = 0.99$; and the red dot is the critical point.

SM 2 SUPPLEMENTARY FIGURES FOR $N = 6$ CASE

helium-4 (${}^4\text{He}$)

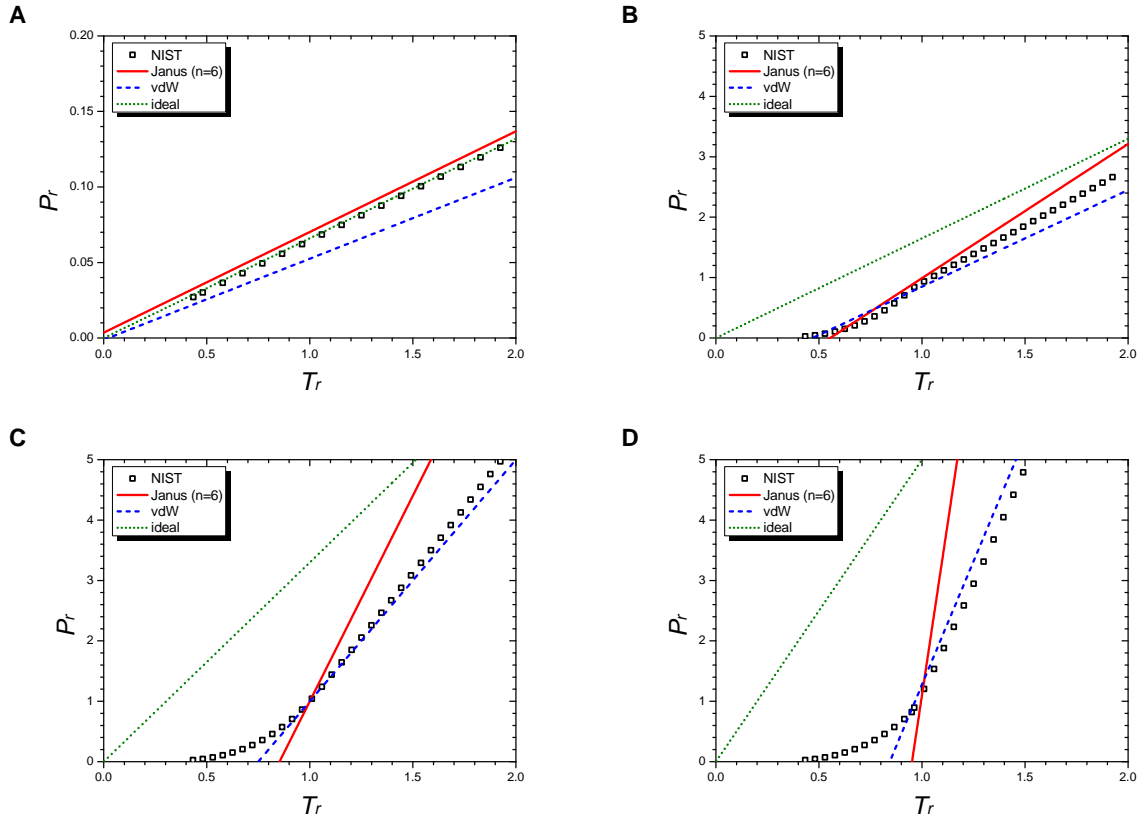


Figure S33. Isochoric curves of helium-4 (${}^4\text{He}$) at $1/v_r = 0.02$ (A), $1/v_r = 0.5$ (B), $1/v_r = 1.0$ (C), and $1/v_r = 1.5$ (D). Boxes are from the NIST data. The red solid line is drawn from the $n = 6$ Janus van der Waals equation, the blue dashed line from the original van der Waals equation, and the green dotted line from the classical ideal gas law.

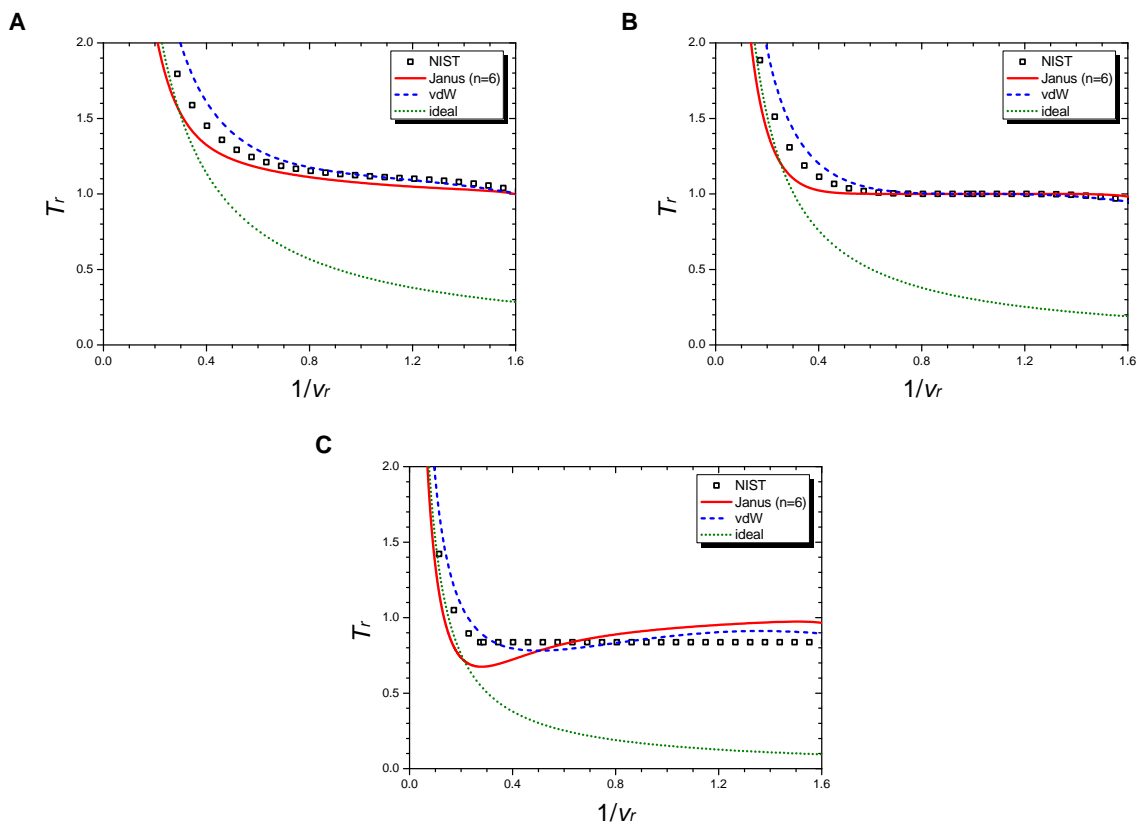


Figure S34. Isobaric curves of helium-4 (${}^4\text{He}$) at $P_r = 1.5$ (A), $P_r = 1.0$ (B), and $P_r = 0.5$ (C). Boxes are from the NIST data. The red solid line is drawn from the $n = 6$ Janus van der Waals equation, the blue dashed line from the original van der Waals equation, and the green dotted line from the classical ideal gas law.

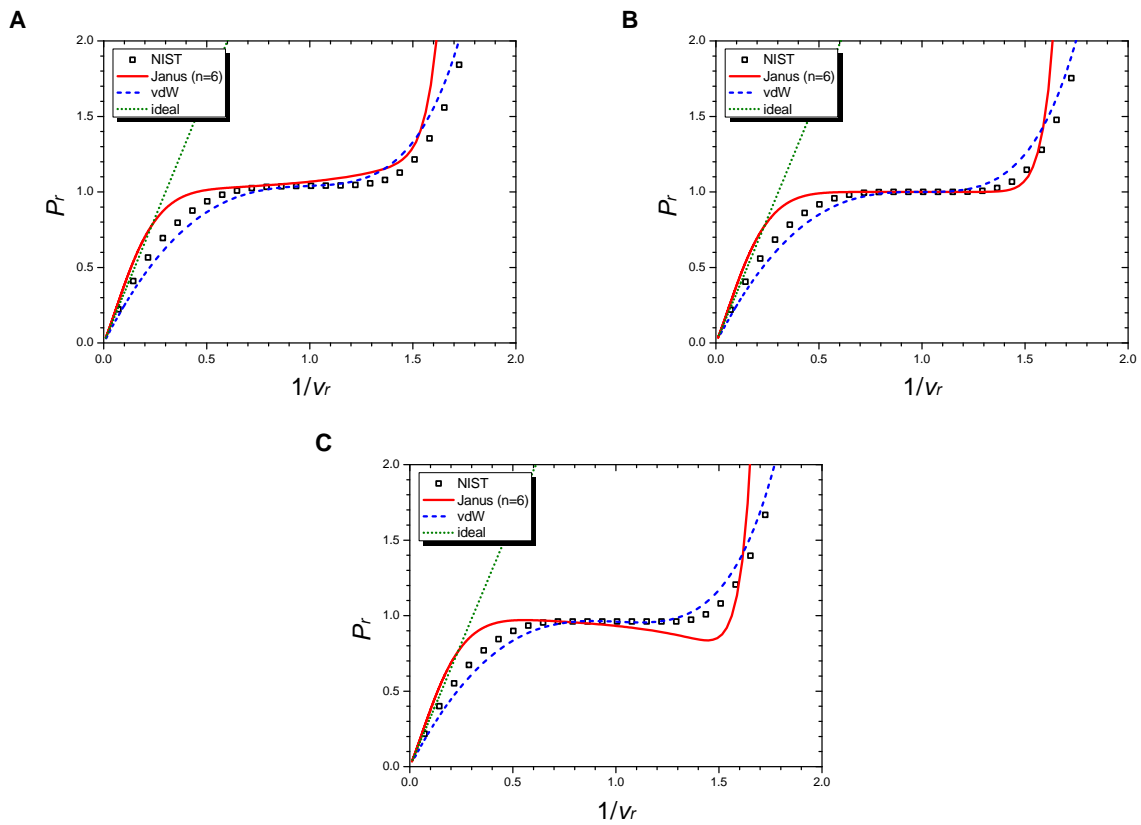


Figure S35. Isothermal curves of helium-4 (^4He) at $T_r = 1.01$ (A), $T_r = 1.00$ (B), and $T_r = 0.99$ (C). Boxes are from the NIST data. The red solid line is drawn from the $n = 6$ Janus van der Waals equation, the blue dashed line from the original van der Waals equation, and the green dotted line from the classical ideal gas law.

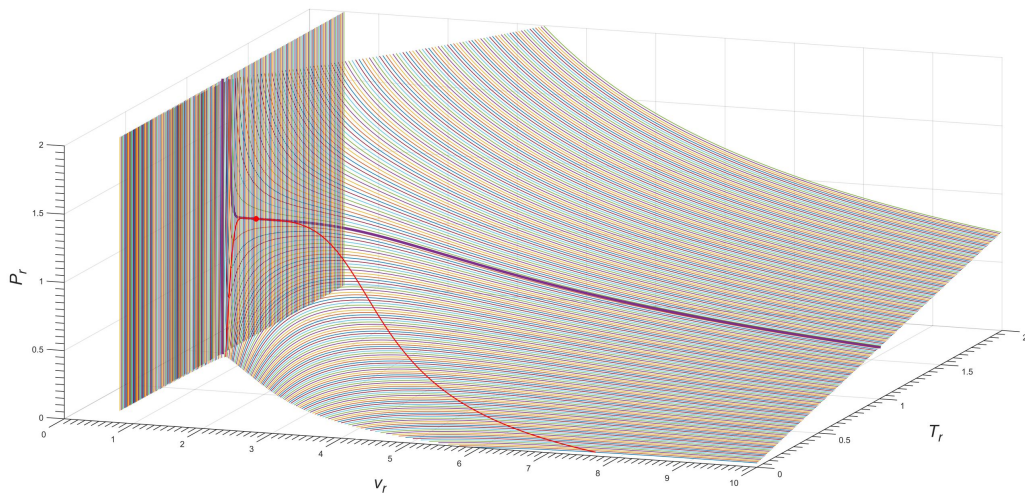


Figure S36. Three-dimensional $P_r - v_r - T_r$ phase diagram of the exact $n = 6$ Janus van der Waals equation, as for helium-4 (${}^4\text{He}$). The bold purple line corresponds to the isotherm of $T_r = 1.00$ as depicted in **Figure S35 B**; the red line is the Janus van der Waals spinodal curve with $a = 0.99$; and the red dot is the critical point.